Acta Pharmaceutica Sinica B 2021;11(7):1835−1852

Chinese Pharmaceutical Association
Institute of Materia Medica, Chinese Academy of Medical Sciences

Acta Pharmaceutica Sinica B

www.elsevier.com/locate/apsb
www.sciencedirect.com

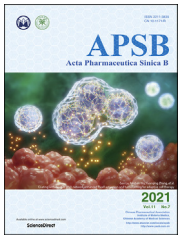

ORIGINAL ARTICLE

Targeted inhibition of GRK2 kinase domain by CP-25 to reverse fibroblast-like synoviocytes dysfunction and improve collagen-induced arthritis in rats

Chenchen Han[a,b], Yifan Li[a], Yuwen Zhang[a], Yang Wang[a], Dongqian Cui[a], Tingting Luo[a], Yu Zhang[a], Qian Liu[a], Hao Li[a], Chun Wang[a], Dexiang Xu[b,*], Yang Ma[a,*], Wei Wei[a,*]

[a]*Institute of Clinical Pharmacology, Anhui Medical University, Key Laboratory of Anti-Inflammatory and Immune Medicine (Anhui Medical University), Ministry of Education, Anhui Collaborative Innovation Center of Anti-inflammatory and Immune Medicine, Hefei 230032, China*
[b]*Public Health and Preventive Medicine Postdoctoral Research Station of Anhui Medical University, Hefei 230032, China*

Received 9 November 2020; received in revised form 28 December 2020; accepted 6 January 2021

KEY WORDS

CP-25;
Rheumatoid arthritis;
Fibroblast-like synoviocyte;
MH7A;
G protein coupled receptor kinase 2;
Prostaglandin E4 receptor

Abstract Rheumatoid arthritis (RA) is an autoimmune disease and is mainly characterized by abnormal proliferation of fibroblast-like synoviocytes (FLS). The up-regulated cellular membrane expression of G protein coupled receptor kinase 2 (GRK2) of FLS plays a critical role in RA progression, the increase of GRK2 translocation activity promotes dysfunctional prostaglandin E4 receptor (EP4) signaling and FLS abnormal proliferation. Recently, although our group found that paeoniflorin-6′-*O*-benzene sulfonate (CP-25), a novel compound, could reverse FLS dysfunction *via* GRK2, little is known as to how GRK2 translocation activity is suppressed. Our findings revealed that GRK2 expression up-regulated and EP4 expression down-regulated in synovial tissues of RA patients and collagen-induced arthritis (CIA) rats, and prostaglandin E2 (PGE2) level increased in arthritis. CP-25 could down-regulate GRK2 expression, up-regulate EP4 expression, and improve synovitis of CIA rats. CP-25 and GRK2 inhibitors (paroxetine or GSK180736A) inhibited the abnormal proliferation of FLS in RA patients and CIA rats by down-regulating GRK2 translocation to EP4 receptor. The results of microscale thermophoresis (MST), cellular thermal shift assay, and inhibition of kinase activity assay indicated that CP-25 could directly target GRK2, increase the protein stability of GRK2 in cells, and inhibit GRK2 kinase activity.

*Corresponding authors. Tel./fax: +86 551 65161209.
E-mail addresses: wwei@ahmu.edu.cn (Wei Wei), mayang_ahmu@126.com (Yang Ma), xudex@126.com (Dexiang Xu).
Peer review under the responsibility of Chinese Pharmaceutical Association and Institute of Materia Medica, Chinese Academy of Medical Sciences.

https://doi.org/10.1016/j.apsb.2021.01.015

The docking of CP-25 and GRK2 suggested that the kinase domain of GRK2 might be an important active pocket for CP-25. G201, K220, K230, A321, and D335 in kinase domain of GRK2 might form hydrogen bonds with CP-25. Site-directed mutagenesis and co-immunoprecipitation assay further revealed that CP-25 down-regulated the interaction of GRK2 and EP4 *via* controlling the key amino acid residue of Ala321 of GRK2. Our data demonstrate that FLS proliferation is regulated by GRK2 translocation to EP4. Targeted inhibition of GRK2 kinase domain by CP-25 improves FLS function and represents an innovative drug for the treatment of RA by targeting GRK2.

1. Introduction

Rheumatoid arthritis (RA) is an autoimmune disease characterized by systemic immune dysfunction and inflammation of the synovial membrane, affecting approximately 0.5%−1% of the population worldwide[1]. The pathological hallmarks of joint synovium in RA is inflammatory immune cells infiltration at the joints, synovial hyperplasia, micro-vessels and pannus formation, eventually leading to articular cartilage and bone erosion and joint destruction, with the high disabilityrate[2,3]. Fibroblast-like synoviocytes (FLS), as the important synovial lining cells, provide structure to the joint by secreting synovial fluid and extracellular matrix. In RA, FLS involve in joint destruction by invading cartilage and promoting inflammation and bone erosion[4].

FLS function is regulated by several different G protein-coupled receptors (GPCRs) signaling involving in protein kinase activation[5−8]. G protein-coupled receptor kinases (GRKs) are crucial regulators of signaling, its role in FLS is still being explored. Our group previously found that GRK2 expression is up-regulated in spleen tissue of adjuvant arthritis (AA) rats[9]. Further studies revealed that GRK2 is a highly expressed protein kinase in FLS and its membrane expression is up-regulated in AA-FLS[7,8].

GRK2, as one of the seven members in the family of serine (Ser)/threonine (Thr) kinase, is a ubiquitously expressed in synovial tissues[10]. It is increasingly clear that GRK2 plays a key regulatory pathological role in the synovial hyperplasia[7,8]. The structure of the 80 kDa protein GRK2 comprises N-terminal domain, kinase domain (KD), and C-terminal domain. N-terminal domain of GRK2 is responsible for mediating receptor recognition and intracellular membrane anchoring[11]. C-terminal domain of GRK2 binds to G$\beta\gamma$ promoting membrane recruitment and subsequent GPCR phosphorylation[12]. KD with some important regions responsible for regulating kinase activity[13]. One mechanism of FLS dysfunction by which continuously increased prostaglandin E2 (PGE2) levels contribute to synovial hyperplasia is through dysregulation of GPCR function in FLS. Enhanced stimulation of prostaglandin E4 receptor (EP4) followed by increased activation of GRK2 leads to enhanced phosphorylation, desensitization and down-regulation of EP4 signaling, promoting FLS dysfunction. The levels and translocation activity of GRK2 are elevated in synovial tissue and synovial cells of AA rats[7,8]. Increased GRK2 translocation activity has been shown to participate in FLS abnormal proliferation during arthritis, whereas GRK2 inhibition through paroxetine that specifically bound to kinase domain of GRK2 could prevent and improve arthritis[14]. These data present compelling evidence of a causal role for GRK2 in synovial hyperplasia leading to arthritis. Therefore, the development of small-molecule inhibitors of GRK2 appears warranted for pharmacologic treatment of RA.

Recently, the clinical drugs used in the treatment of RA mainly include non-steroidal anti-inflammatory drugs, steroidal anti-inflammatory drugs, disease modifying antirheumatic drugs (DMARD), biological agents, etc. Although the current drugs for treating RA can improve the pathological manifestations of RA patients, there are still many adverse drug reactions (ADR). Methotrexate (MTX) is the most widely used DMARD, which remains the gold standard and the cornerstone of DMARD-based RA treatment. However, MTX in treating RA patients has a dose−response relation exists, and higher MTX doses are more prone to result in ADR[15−18]. Although biological agents, including rituximab and etanercept, have had a major impact on the therapy of RA, they do not yet resolve all the clinical problems due to their inconsistent efficacy and comorbidities, including increased risk of infections and tumors[19−23]. Therefore, it is necessary to better understand the pathogenesis of RA and develop new molecularly targeted agents to improve the clinical performance of RA patients and reduce ADR.

Paeoniflorin-6′-*O*-benzene sulfonate (code: CP-25; chemical formula: $C_{29}H_{32}O_{13}S$; molecular weight: 620.62; Chinese patent number: ZL201210030616.4), as a novel ester compound, is esterification modification of paeoniflorin which is an active ingredient extracted from the roots of *Paeonia lactiflora* Pall. with anti-inflammatory and immunomodulatory effects[24,25]. Compared the therapeutic effect of CP-25 and MTX in collagen-induced arthritis (CIA) or AA rats, our studies found that both CP-25 and MTX are against joint damage, including cartilage and bone erosion, cellular infiltration, and synovial proliferation. However, MTX results in various side effects, including obvious signs of weight loss, loss of appetite, and lack of movement, which may be due to cytotoxicity, whereas no such symptoms are detected in CP-25-treated rats, indicating that CP-25 is well tolerated at the tested doses[26]. Compared the therapeutic effect of CP-25, etanercept, and rituximab on B cell functions, our group found that CP-25 down-regulates the percentage of total B cells, the activate B cells and the plasma cells, and moderately activate B cell subsets to the normal level. However, rituximab and etanercept exerted severe inhibition effects on B cell function, leading to the dysfunction and apoptosis of B cells, which was one of mechanisms of ADR for biological agents in the treatment of autoimmune diseases[27,28]. Compared the effect of CP-25 and MTX on FLS abnormal proliferation, our group found that CP-25 regulates PGE2−EP4−cAMP signaling to mediate FLS abnormal proliferation by inhibiting GRK2 translocation to EP4, but MTX does not inhibit GRK2 translocation to the membrane[8]. Structural analysis

found that CP-25 with cyclohexane and two oxygen heterocyclic rings was similar to the benzodioxole ring of GRK2 inhibitor paroxetine, suggesting that CP-25 may bind to some amino acids of kinase domain in GRK2 to exert the regulation of GRK2 activity. All these data suggest a possible role of CP-25 in improving immune cells and FLS function by targeting GRK2. Nevertheless, the mechanistic role of CP-25 binding to kinase domain of GRK2 to inhibit EP4 desensitization mediated FLS abnormal proliferation was not explored so far.

Here, we found that GRK2 expression up-regulated during synovial tissues of RA patients and CIA rats, and FLS abnormal proliferation of RA patients and CIA rats was regulated by GRK2 translocation to EP4. CP-25 specifically bound to the kinase domain of GRK2, inhibited kinase activity in the micromolar range of affinity, and down-regulated GRK2 translocation by controlling GRK2 Ala321, thereby inhibiting FLS abnormal proliferation and improving synovitis. Finally, we show that CP-25, target to GRK2, has therapeutic potential for CIA rats by inhibiting FLS abnormal proliferation.

2. Materials and methods

2.1. Patients and specimens

RA synovial tissue samples were obtained from RA patients diagnosed by the criteria of American College of Rheumatology, and they were undergoing surgical synovectomy of the knee. Normal synovial samples were obtained from patients with noninflammatory knee joint diseases, and they were generally derived from trauma patients undergoing lower limb amputation, and patients with bone tumor undergoing lower extremity amputation. All patients gave their informed consent, and the study protocol was approved by Biomedical Ethic Committee of Anhui Medical University (No. 20131321, Hefei, China).

2.2. Animals

Wistar rats aged 6−7 weeks, with the weight of (150±20 g), were purchased from the Beijing Vital River Laboratory Animal Technology Co., Ltd. (Beijing, China). The mice were housed under standard laboratory conditions. All research adhered to the principles of the laboratory animals care guidelines and was approved by Biomedical Ethic Committee for Animal Experimentation of Anhui Medical University (No. 20131321, Hefei, China).

2.3. Drugs and reagents

CP-25 [$C_{29}H_{32}O_{13}S$, molecular weight: 620] white crystalline powder, purity>98%, was provided by the Chemistry Laboratory of the Institute of Clinical Pharmacology of Anhui Medical University (Hefei, China); GSK180736A (Cat. HY-18990) was obtained from MedChemExpress (USA). PGE2 (Cat. 14010) and CAY10598 (Cat. 13281) were purchased from Cayman Chemical (USA). Paroxetine was purchased from Zhejiang Huahai Pharmaceutical Co., Ltd. (China). MTX (2.5 mg per tablet) was purchased from XINYI Medical Ltd., Co. (China) in Shanghai. Chicken collagen II (CCII) was obtained from Chondrex Corp. (USA). Bacille calmette-guerin (BCG) was purchased from Beijing Biologicals Institute (China). Enzyme-linked immunosorbent assay (ELISA) kits for PGE2 and transforming growth factor β (TGF-β) were the products from Raybiotech, Inc. and Nanjing Fcmacs Biotech Co., Ltd. Luminex assay for tumor necrosis factor α (TNF-α), granulocyte-macrophage colony-stimulating factor (GM-CSF), interleukin (IL)-1β, IL-6, interferon γ (IFN-γ), vascular endothelial growth factor (VEGF), and intercellular adhesion molecule 1 (ICAM-1) were the products from Raybiotech, Inc. Fluorescein isothiocyanate (FITC)-CD3, allophycocyanin (APC)-CD4, phycoerythrin (PE)-IL-17, PE-CD25, eFluor 450-forkhead box P3 (Foxp3), and regulatory T cell detection kit were procured from eBioscience, Inc. Alexa-Fluor-488- and Alexa-Fluor-594-tagged second antibodies were obtained from Proteintech. Secondary antibodies, β-actin, EP4 (sc-55596), GRK2 (sc-562), protein A/G plus-agarose (sc-2003), normal rabbit lgG (sc-2027), and GRK2 Alexa Fluor 488 (sc-13143 AF488) were purchased from Santa Cruz Biotechnology. Dimethylsulfoxide (DMSO) was obtained from Sigma−Aldrich. ATP1alpha1/Na^+K^+ATPase1 (ATP1A1) was purchased from ZSGB-BIO. GRK2 protein was purchased from Thermo Fisher Scientific. Transwell chambers and Matrigel were purchased from Corning Costar. 647-Vimentin (CST, Cat. 9856). ADP-Glo™ Kinase Assay (Promega, Cat. V9351). GRKtide (Signalchem, Cat. G46-58).

2.4. Establishment of CIA model of rats

The CIA model of rats was induced according to the protocol described previously[29]. Briefly, CCII was dissolved in 0.01 mol/L filtered acetic acid by grinding on ice, and the concentration of CCII reached 4 mg/mL. Meanwhile, BCG (50 mg/branch), with water bath heating at 80 °C for 1 h, and was dissolved in sterile liquid paraffin by grinding on ice, and the concentration of BCG reached 6 mg/mL. The CCII was mixed and emulsified thoroughly with the same volume of BCG. A total of 0.2 mL emulsion was injected intradermally into the base of the tail or back at multiple sites. Seven days later, the same emulsion was made and the rats were given a booster injection. The first immunization day was defined as Day 0. After the onset of CIA (around Day 17), model rats were randomly divided into CIA group, CP-25 group, paroxetine group, and MTX group, according to the clinical scores. CP-25 (50 mg/kg/day), paroxetine (15 mg/kg/day), and MTX (0.5 mg/kg/3 days) were dissolved in 0.5% CMC-Na and administered by gavage for 21 days.

2.5. Evaluation of arthritis

The rats were inspected every three days following the established standard from the onset of secondary inflammation[30]. The body weight, global assessment, arthritis index, swollen joints count, and paw swelling were recorded and analyzed.

2.6. Histological examination

The rats were anesthetized and killed at the end of the experimental period, the joints, and spleen were fixed in 4% paraformaldehyde and then embedded in paraffin. Sections (5 mm) were stained with hematoxylin and eosin (HE), and were examined microscopically. Representative micrographs of HE-stained histological sections of the joints and spleen are shown. The histology section shows the synoviocytes (S), the pannus (P), the inflammatory cells (I), the bone (B), and the cartilage (C). The grading scheme consisted of ordinal categories ranging from 0 (no effect) to 3 (severe effect)[31]. The spleen was evaluated by examining the white pulp (W), the red pulp (R), the marginal zone

(MZ), the germinal center (GC), and the periarteriolar lymphoid sheaths (PALS). The grading scheme consisted of ordinal categories ranging from 0 (no effect) to 3 (severe effect)[32].

2.7. Determination of lymphocytes vitality

The vitality of lymphocytes of spleen or thymus was determined using CCK-8 kit according to the instructions. 100 μL of 1×10^5/mL lymphocytes were placed to 96 well plates in serum free media. 10 mg/mL concanavalin A (ConA) or lipopolysaccharide (LPS) was used to stimulate lymphocytes for 48 h. Four hours before the end of the culture, 10 μL of CCK-8 was added into individual well, the plate was read on a microplate reader at 450 nm. Each sample was conducted in triplicate.

2.8. Flow cytometry

PBMCs or lymphocytes of spleen were separated into different tubes and stained with FITC-CD3, APC-CD4, PE-IL-17, PE-CD25, and PB450-Foxp3. Regulatory T cells were detected by a Treg kit (APC-CD4, PE-CD25, and PB450-Foxp3) according to the manufacturer's directions. As previously described[33], GRK2 and EP4 antibodies were added in FLS, the samples were tested with a flow cytometer (FC500, Beckman) and the results were analyzed using CytExpert (Beckman).

2.9. Cytokines detection

Serum samples, spleen tissue, and the supernatant fluid of FLS were extracted from rats. The expression of TNF-α, GM-CSF, IL-1β, IL-6, IFN-γ, VEGF, and ICAM-1 was detected by Luminex assay according to the instructions of the manufacturers. The expression of PGE2 and TGF-β was detected by ELISA. The plates were read under 450 nm, and each sample was duplicated.

2.10. Immunohistochemistry (IHC)

Synovial tissues were deparaffinized in xylene and rehydrated in ethanol. After that, 0.5% Triton X-100 [polyethylene glycol mono (p-1,1,3,3-tetramethyl butyl) phenyl ether] was used for 30 min to permeate cell. Then after rinsed in phosphate-buffered saline (PBS), the sections were incubated with Tris-EDTA for 10 min. Afterwards, following a 15 min hydrogen peroxide (3%) incubation, endogenous peroxidase activity was destroyed. After a rinse of PBS, the sections were incubated with GRK2 antibody/EP4 antibody overnight at 4 °C Then the sections were incubated with polymer helper after rinse of PBS for 20 min at 37 °C. After that, the incubation with polyperoxidase-anti-mouse/rabbit IgG was proceeded for 30 min at 37 °C. Finally, the specimens were conducted with 3,3′-diaminobenzidine tetrahydrochloride and then counterstained with hematoxylin. All images were captured by an optical microscope.

2.11. Confocal microscopy

Synovial tissues were incubated overnight at 4 °C with monoclonal anti-GRK2 and anti-EP4 antibodies in synovial tissues. Synovial tissues were washed with PBS, and then they were incubated for 2 h at room temperature with Alexa-Fluor-488- or Alexa-Fluor-594-tagged second antibodies.

FLS was cultured in 35-mm glass-bottom dishes, fixed with 4% paraformaldehyde, permeabilized with 0.1% Triton X-100, and then blocked with 0.5% bovine serum albumin (BSA). The cells were then incubated with anti-GRK2 and anti-EP4 antibodies overnight in a 4 °C wet chamber. After washing with PBS, samples were incubated with anti-rabbit-Alexa Fluor 488 and antimouse-Alexa Fluor 594 for 1 h at 37 °C. Images of the fluorescent signal were acquired under a TCS SP8 confocal microscope (Leica Microsystems).

2.12. FLS culture and identification

FLS were isolated from synovial tissues. Cultures were maintained in Dulbecco's modified Eagle medium (DMEM) supplemented with 20% fetal bovine serum (FBS), penicillin (100 units/mL) and streptomycin (100 μg/mL) in an incubator at 37 °C with 5% CO_2. Synoviocytes were cultured with Anti-647-Vimentin for 30 min, detected by a flow cytometer and the results were analyzed using CytExpert, positive rate of Vimentin more than 90% in synoviocytes diagnosed as FLS.

2.13. FLS proliferation

FLS were counted and seeded onto 96-well plates at a density of 5×10^3 cells/well. Cells cultured for 48 h at 37 °C with 5% CO_2. After washing with PBS, samples were incubated with 20 μL of diaminophenyl indole (DAPI) for 5 min. Fluorescent images were taken with an ImageX press micro four high content imaging system (Molecular Devices).

2.14. Small interfering RNA (siRNA)

Grk2 siRNAs were chemically synthesized by Genepharma Co., Ltd. (Shanghai, China) to knockdown *Grk2* in FLS as follows: negative control (sense: 5′-UUCUCCGAACGUGUCACGUTT-3′, anti-sense: 5′-ACGUGACACGUUCGGAGAATT-3′); *Grk2*-rat-796 (sense: 5′-CCAUGAAGUGUCUGGACAATT-3′, anti-sense: 5′-UUGUCCAGACACUUCAUGGTT-3′).

FLS were transfected at 70% confluency in 24-well plates using siRNA-mate according to the manufacturer's protocol. After 48 h, silencing of *Grk2* was confirmed *via* Western blot from our previous study[7].

2.15. Isolation of proteins from the cytoplasm and the membrane

FLS were lysed and centrifuged at 12,000×*g* for 15 min at 4 °C. Some of the supernatant was centrifuged at 100,000×*g* for 60 min at 4 °C. The precipitate containing the membrane proteins was resuspended in cell lysis buffer containing 1 mmol/L phenylmethanesulfonyl fluoride (PMSF), then the supernatant was analyzed, which to detect GRK2 and EP4. The protein concentration was determined using the bicinchoninic acid (BCA) protein assay.

2.16. Western blot

The proteins were electrophoresed on 10% SDS-polyacrylamide gel electrophoresis (PAGE) gels at 110 V for 1.5 h and proteins were transferred to PVDF membranes at 200 mA for 2 h. The membrane was incubated with 5% fat-free milk in phosphate buffer saline with tween-20 (TPBS) for 2 h at room temperature.

The membranes were incubated and probed with the first antibody at 4 °C overnight according to manufacturer's instructions and followed by the addition of secondary antibody, followed by visualization of the proteins with imageQuant Las 4000 mini (Sigma), and the density of each band was quantified using Photoshop CS5 (Adobe). Protein quantification was normalized to the corresponding levels of β-actin or ATP1alpha1/Na^+K^+ATPase1, which were not altered dramatically between the different treatment conditions. Each blot is a representative of at least three similar independent experiments.

2.17. Co-immunoprecipitation assay

Whole-cell lysate IP was performed by lysing cells in the lysis buffer: 25 mmol/L hydroxyethyl piperazine ethylsulfonic acid (HEPES), 150 mmol/L NaCl, 5 mmol/L EDTA, 1% Triton X-100, 10% (*v*/*v*) glycerin, protease inhibitors, and phosphatase inhibitors. The lysate was kept on ice for 30 min and insoluble material was removed by centrifugation with 12,000×*g* for 15 min at 4 °C. Lysates were precleared using normal mouse lgG for 2 h at 4 °C. Antibodies were added to protein A/G plus-agarose for 2 h at 4 °C, with precleared lysates incubated at 4 °C overnight. The immune complexes were collected using protein A/G plus-agarose and beads were washed three times extensively with the lysis buffer. To denature proteins, lysates were added to 5 × reducing SDS-PAGE loading buffer and heated to 95 °C for 10 min. Protein levels were assessed by standard SDS-PAGE and transferred to PVDF membranes. The bands were then visualized with imageQuant Las 4000 mini. The density of each band was quantified using Photoshop CS5.

2.18. Data analysis and label-free quantitation

As described previously[34], Label-free quantitative protein analysis is a proteomics data analysis method based on mass spectrometry (MS) detection platform. The basic process of hierarchical clustering analysis of differentially expressed proteins is as follows: first, the normal differential correction of the differentially expressed protein expression values obtained from each group of comparison is used as the input of the hierarchical clustering algorithm. The distance is Euclidean distance, and the linkage is Complete Linkage Method. Finally, a hierarchical cluster analysis heat map is obtained.

The Gene Ontology (GO) database (geneontology.org) contains functional information on the biological processes involved in genes, the location of cells, and the molecular functions they play. In this project, we map genes to each node of the GO database and use GO (http://www.geneontology.org/) for functional enrichment analysis. Differentially expressed proteins compared in each group are classified and displayed in three independent ways: Biological Process (GO_BP), Cellular Component (GO_CC), and Molecular Function (GO_MF).

The Kyoto Encyclopedia of Genes and Genomes (KEGG) Pathway Database (www.kegg.jp/kegg/pathway.html) store functional information of genes and genomes, including illustrated cellular biochemical processes, such as metabolism, membrane transport, signaling, cell cycle, and conserved sub-pathways. By analyzing the metabolic pathways in which differentially expressed proteins are significantly enriched, one can understand which pathways have undergone significant systemic changes under different experimental conditions. The results were rendered using the mapping module provided by the KEGG website searching the *Rattus norvegicus* (rat) database for differentially expressed protein expression content rendering.

2.19. Microscale thermophoresis (MST)

As described previously[35], the equilibrium dissociation constant (K_d) values were measured using the Monolith NT.115 instrument (NanoTemper Technologies). The proteins were fluorescently labeled according to the manufacturer's protocol. A range of concentrations of compounds such as CP-25, paroxetine (from 5 nmol/L to 1 mmol/L) were incubated with 200 nmol/L of purified labeled GRK2 protein (Invtrogen) for 10 min in assay buffer (50 mmol/L Tris-HCl, 100 mmol/L NaCl, pH 7.5). The sample was loaded into the NanoTemper glass capillaries and microthermophoresis was carried out using 80% light emitting diode (LED) power and 80% MST. The K_d values were calculated using the mass action equation *via* the NanoTemper software from duplicate reads of triplicate experiments. Paroxetine, as GRK2 inhibitor, is positive control in the experiment.

2.20. Docking of CP-25 to the GRK2 structural model

Docking simulation of CP-25 with GRK2 protein (PDB ID: 3KRW) was carried out with the program Discovery Studio 2.1 (DS 2.1, Accelrys Software Inc.). The active sites were defined and sphere of 10 Å according to the reported important amino acid residues of GRK2, which generate around the active site pocket, with the active site pocket of BSAI model using C-DOCKER, a molecular dynamics (MD) simulated-annealing based algorithm module from DS 2.1. As previously described[36], the structure of protein, substrate was subjected to energy minimization using CHARM force field as implemented in DS 2.1. A full potential final minimization was then used to refine the substrate poses. Based on C-DOCKER, energy docked conformation of the substrate was retrieved for post-docking analysis.

2.21. Thermal shift assay

In vivo cellular thermal shift assay (CETSA): HepG2 cells (1×10^7) were seeded into a 100 mm culture plate with 10^{-6} mol/L of CP-25 or paroxetine and cultured for 2 h. GRK2-WT and GRK2-G201A/A321G/D335A/K220R/K230R plasmids were transiently transfected to HEK 293T cells with Lipofectamine 3000 (Invitrogen). Transfection of HEK 293T cells was performed 48 h according to the manufacturer's protocol, and cells cultured with 10^{-6} mol/L of CP-25 or paroxetine for 2 h. As previously described[37], control cells were incubated with the same volume. Cells were cultivated and counted, followed by resuspending in PBS (containing 1 mmol/L PMSF) to a final density of 2×10^7/mL. Then cells were subpackaged into seven PCR tubes, with 100 μL per PCR tube, and heated with a thermal gradient from 37 to 67 °C for 3 min. After freeze−thawed twice with liquid nitrogen, the supernatant was separated by centrifugation at 12,000×*g* for 20 min and collected. 20 μL of the supernatant was loaded onto an SDS-PAGE gel, followed by an immunoblot.

2.22. GRK2 kinase assay

GRK2 kinase enzyme was detected by ADP-Glo Kinase Assay Kit and performed the experiment as per manufacturer's protocol. The GRK2 inhibition assay was performed with the ADP-Glo system using 200 ng of GRK2, 0.5 μg of GRKtide substrate, 25 μmol/L

ATP, and the different concentration of CP-25 or GSK180736A for 120 min. As previously described[38], after the initial reaction, ADP-Glo reagent was added to the reaction and allowed to incubate for an additional 40 min. Lastly, the kinase detection reagent was added and allowed to incubate for 30 min, and the luminescence was measured with automatic microplate reader (TECAN GENIOS). All data was analyzed, and inhibition curves were fit *via* GraphPad Prism software.

2.23. Construction of *GRK2* mutant plasmids and cell line

The coding sequence of *GRK2* in pGEM-T-vector was obtained from previously construction. Site-directed mutagenesis was performed to obtain G201A, K220R, K230R, A321G, and D335A by TaKaRa MutanBEST Kit (TaKaRa). *GRK2* mutants were amplified by PCR, and the sequences of the forward and reverse primers were as follows: *GRK2*G201A, forward 5′-GGGCCTTTGGCGAGGTCTATGG-3′, reverse 5′- TTGCCTGTGTCAGCCTTCCGGCAC-3′; *GRK2*K220R, forward 5′-TGAGGTGCCTGGACAAAAAGCGCATC-3′, reverse 5′-TGGCGTACATCTTGCCTGTGTCAGCCT-3′; *GRK2*K230R, forward 5′-CATCAAGATGAGGCAGGGGGAGACC-3′, reverse 5′- AGAGCATGATGCGCTCGTTCAGGGCCAG-3′; *GRK2*A321G, forward 5′-CATCCTTCTGGACGAGCATGGCCACGT-3′, reverse 5′-TTGCCTGGCTTCAGGTCCCGGTAGACCACG-3′; *GRK2*D335A, forward 5′-GGGCCTGGCCTGTGACTTCTCCAAGAAG-3′, reverse 5′-AGGGCCGAGATCCGCACGTGGCCAT-3′.

The PCR fragments were subcloned into the Sal I and Apa I sites of the pEGFP-C3 vector, then pEGFP-C3-*GRK2* mutants were cloned into the BamH I and Sal I sites of the pIRES-EGFP vector. The coding sequence of every construct was verified. The plasmids were transiently transfected to HEK 293T cells with Lipofectamine 3000. Transfection of HEK 293T cells was performed 48 h according to the manufacturer's protocol. Unless stated otherwise, transfection of *GRK2* was performed using 2.5 μg of *GRK2* plasmid DNA in 6-well plates. The transfection effect was observed by LX-70 fluorescent inverted microscope (OLYMPUS).

2.24. Statistical analysis

The data are expressed as mean ± standard deviation (SD) of at least three separate experiments in triplicate. Analysis of variance (ANOVA) (SPSS software products, USA) was used to determine significant differences between groups, *t*-test was applied for the comparison between two groups and significance was established at a $P < 0.05$. Data were carried out using GraphPad Prism.

3. Results

3.1. GRK2 membrane expression in synovial tissues of RA patients and CIA rats

Our group reported that GRK2 membrane expression increased in PGE2-induced FLS dysfunction[7]. In the attempt to identify whether GRK2 expression regulates the change of synovial pathology in RA, we assessed pathological feature of synovial tissues in RA patients by HE and detected proteins expression, and discovered that compared with normal group, synovial tissues of RA patients (Fig. 1A) have obviously synovial hyperplasia, with increase of FLS cell density, pannus formation, and inflammatory cell infiltration. Compared with the normal group, GRK2 expression in synovial tissue of RA patients significantly increased, EP4 expression significantly decreased, and the association of GRK2 and EP4 increased (Fig. 1B−D), suggesting that GRK2 translocation to EP4 may be involved in synovial hyperplasia of RA patients.

To further reveal the role of GRK2 expression in the change of synovial pathology of CIA rats and the effects of CP-25, we established CIA rat arthritis model, and treated with CP-25, paroxetine (GRK2 inhibitor), and MTX, then assessed pathological feature of synovial tissues in CIA rats by HE and detected proteins expression. The results showed that normal synovial tissues have one to three layers of synoviocytes. However, histopathologic features of synovial tissues in CIA group encompass synovial hyperplasia, large amounts of lymphocyte infiltration, pannus formation, and destruction of cartilage and bone. CP-25 and paroxetine relieve the arthritis of CIA rats, reduce synovial hyperplasia and FLS cell density (Fig. 2A); compared with CIA group, CP-25 and paroxetine treatment down-regulate GRK2 expression and up-regulate EP4 expression (Fig. 2B and C), suggesting that CP-25 down-regulates GRK2 expression and restores EP4 expression in synovial tissue of CIA rats.

To comprehensive evaluate the therapeutic effects of CP-25, paroxetine, and MTX in CIA rats, we also examined clinical manifestation in CIA rats and the effect of CP-25. The paw swelling, global assessments, arthritis index, and swollen joint count of CIA rats were reduced to varying degrees in the treatment of CP-25, paroxetine, and MTX (Supporting Information Fig. S1). CP-25, paroxetine, and MTX treatment helped improved pathological of spleen, inhibited spleen and thymus index, and lymphocyte of spleen and thymus proliferation (Supporting Information Fig. S2), participated in regulating the percentage of Th17 and Treg in peripheral blood mononuclear cell (PBMC) and spleen (Supporting Information Fig. S3), inhibited secretion of pro-inflammatory cytokines in serum and spleen, such as PGE2, TNF-α, IL-1β, IL-6, IFN-γ, GM-CSF, ICAM-1, and VEGF, and up-regulated the expression of anti-inflammatory cytokines TGF-β (Supporting Information Fig. S4). Collectively, our data reveal that CP-25 has anti-inflammatory and immunomodulatory effects on CIA rats.

3.2. CP-25 inhibits EP4 desensitization mediated FLS abnormal proliferation by down-regulating GRK2 translocation

It has been reported that PGE2-induced GRK2 transloction to EP4 by cAMP−PKA signaling pathway in FLS[7]. To determine what induces GRK2 translocation during chronic arthritis, we considered the release of inflammatory factors in FLS during chronic arthritis. We isolated primary synoviocytes from rats, and identified by flow cytometry, and the expression of Vimentin in cells was more than 90%, which was identified as FLS (Supporting Information Fig. S5A). We next screened 34 differential proteins from FLS with the treatment of CP-25 by label analysis, CP-25 down-regulated 33 proteins, including Anxa2, Anxa5, Anxa6, Arf 1, Atp5f1b, Capg, Ckb, Crk, Ctsd, Ctsh, Eif4a2, Eno 1, Fkbp1a, Hexb, Hmgb1, Hnrnpa2b1, Hsp90ab1, Hspa5, Ldha, Mif, Pdia3, Pgk1, Prdx2, Ptges3, Rack 1, S100a10, S100a11, S100a4, Sod 2, Sparc, Stip1, Txn, and Vcp, and up-regulated Oat protein (Supporting Information Fig. S5B), those proteins involved in promoting joint inflammation, synoviocytes proliferation, and migration, and regulating the release of pro-inflammatory mediators, including PGE2, TNF-α, IL-1β, IL-6, etc.[39−44]. The result

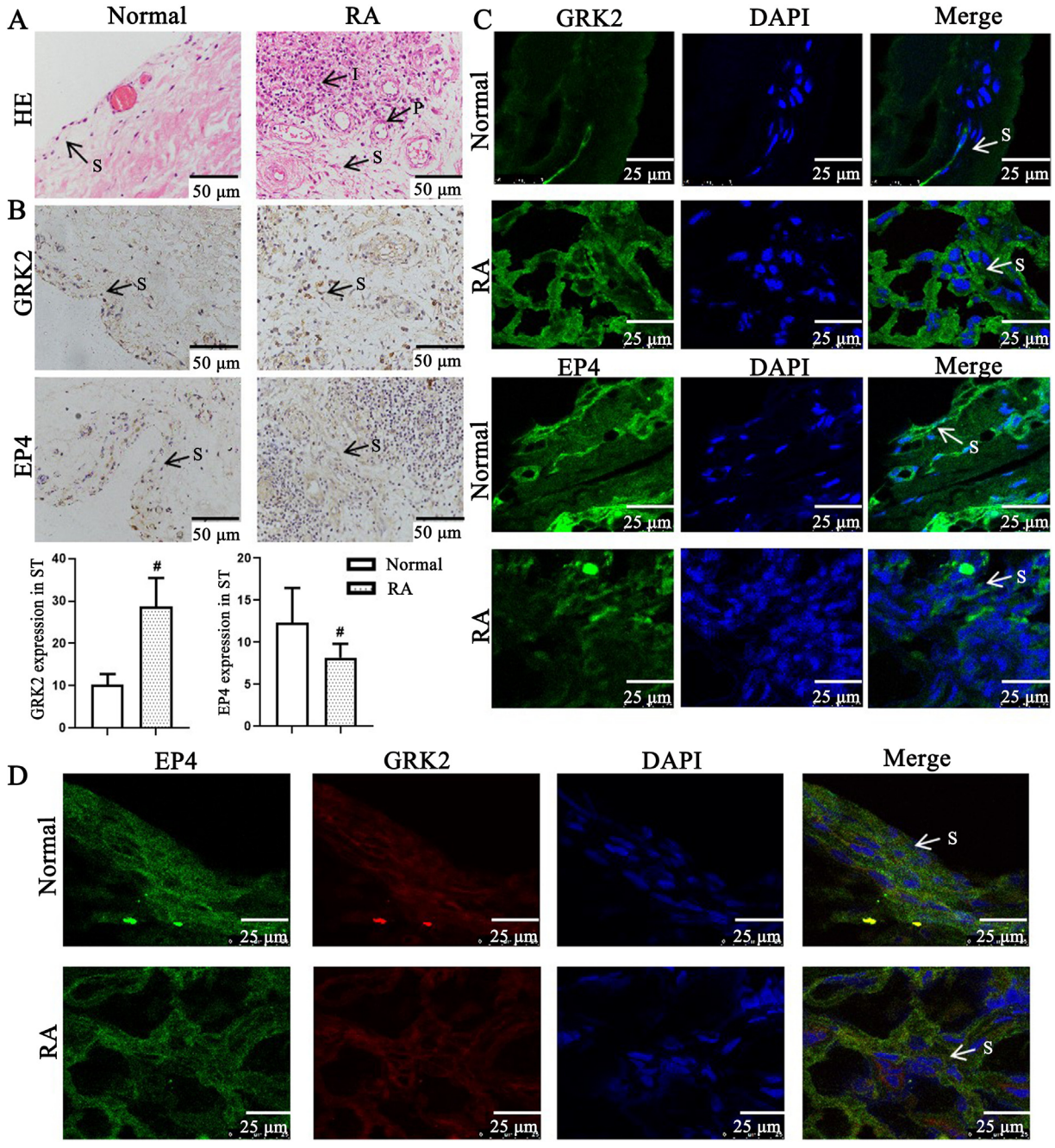

Figure 1 G protein coupled receptor kinase 2 (GRK2) and prostaglandin E4 receptor (EP4) expression in synovial tissues (ST) of rheumatoid arthritis (RA) patients. (A) Representative micrographs of haematoxylin and eosin (HE)-stained histological sections of synovial tissues. The histology section shows the synoviocytes (S), the pannus (P), the inflammatory cells (I) ($n = 8$). Scale bars = 50 μm. (B) GRK2 and EP4 expression in synovial tissues paraffin section of RA patients were detected by immunohistochemistry ($n = 8$). Data are expressed as mean ± standard deviation (SD). $^{\#}P < 0.05$ *vs.* normal group. Arrows indicated the fibroblast-like synoviocytes (FLS) of RA. Scale bars = 50 μm. (C) GRK2 and EP4 expression in synovial tissues paraffin section of RA patients were detected by laser scanning confocal microscope ($n = 8$). Arrows indicated the FLS of RA. Scale bars = 25 μm. (D) GRK2/EP4 expression in synovial tissues frozen section of RA patients were detected by laser scanning confocal microscope ($n = 8$). Arrows indicated the FLS of RA. Scale bars = 25 μm.

of GO analysis (Supporting Information Fig. S5C) and KEGG pathway analysis (Supporting Information Fig. S5D) showed these proteins mainly located in cytoplasm, were most frequently related to the regulation of molecular function, involved in MHC protein binding, protein binding, and participated in antigen processing and presentation, HIF-1 signaling pathway, and protein processing in endoplasmic reticulum. Further research found that inflammatory factors including PGE2, TNF-α, IL-1β, IL-6, IFN-γ, GM-CSF, ICAM-1, VEGF, and TGF-β are increased in the supernatant fluid of FLS in CIA group. CP-25, paroxetine, and MTX inhibited PGE2, TNF-α, IL-1β, IL-6, IFN-γ, GM-CSF, ICAM-1, VEGF, and TGF-β in the supernatant fluid of FLS (Supporting

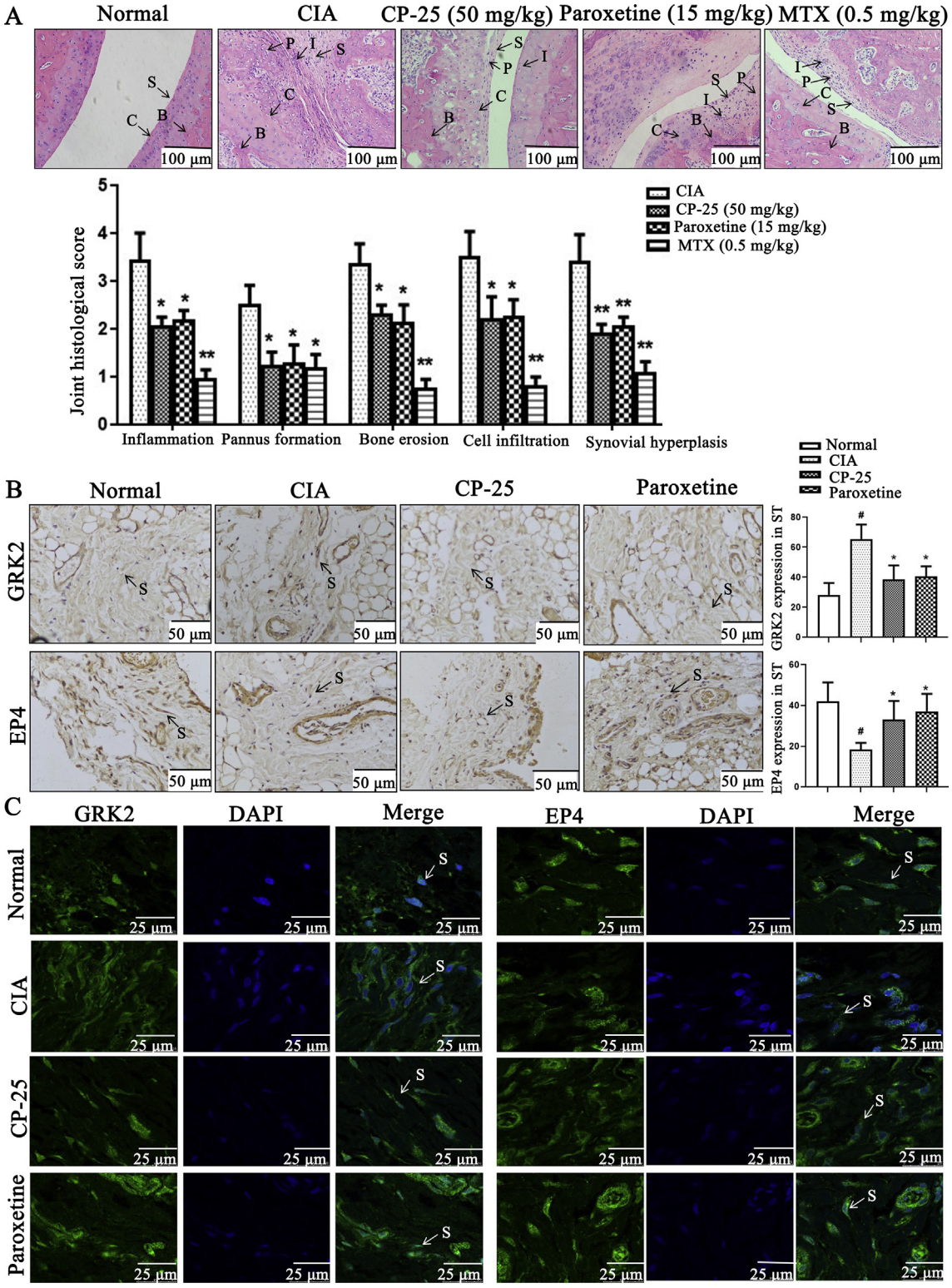

Figure 2 GRK2 and EP4 expression in synovial tissues of CIA rats. (A) Representative micrographs of HE-stained histological sections of the joints are shown. The histology section of the joints shows the synoviocytes (S), the pannus formation (P), the inflammatory cells (I), the bone (B), and the cartilage (C) ($n = 6$). Data are expressed as mean ± SD. $^{*}P < 0.05$, $^{**}P < 0.01$ *vs.* CIA group. Scale bars = 100 μm. (B) The effect of CP-25 on the expression of GRK2 and EP4 in the synovial cells of CIA rats was detected by immunohistochemistry assay ($n = 6$). Arrows indicated the FLS of CIA rats. Scale bars = 50 μm. (C) The effect of CP-25 on the distribution of GRK2 and EP4 in the synovial cells of CIA rats was detected by laser scanning confocal microscope ($n = 6$). Arrows indicated the FLS of CIA rats. Scale bars = 25 μm. Data are expressed as mean ± SD. $^{\#}P < 0.05$ *vs.* normal group; $^{*}P < 0.05$, $^{**}P < 0.01$ *vs.* CIA group.

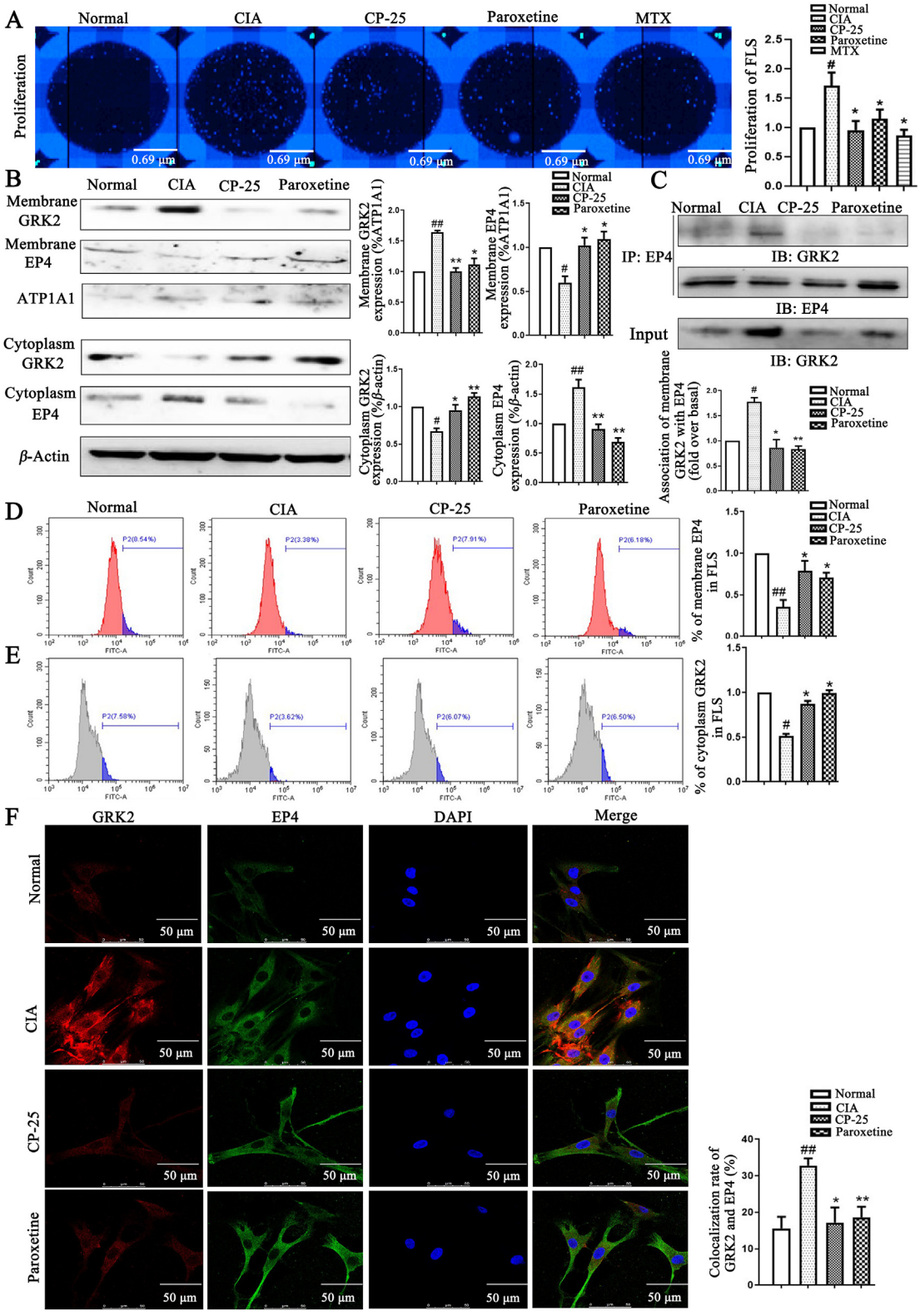

Figure 3 CP-25 treatment improves FLS proliferation of CIA rats by down-regulating GRK2 translocation. (A) CP-25 inhibited FLS abnormal proliferation was detected by high content cell imaging system ($n = 6$). (B) The effect of CP-25 on the expression of GRK2 and EP4 on membrane and cytoplasm of FLS ($n = 4$). (C) FLS lysates were used anti-EP4 antibody by co-immunoprecipitate and subjected to Western blot to visualize GRK2 to evaluate the association with EP4 ($n = 4$). (D) EP4 membrane expression of FLS by flow cytometry ($n = 6$). (E) GRK2 cytoplasm expression of FLS by flow cytometry ($n = 6$). (F) The co-expression of GRK2 and EP4 was detected by laser confocal microscopy ($n = 6$). Scale bars = 50 μm. Data are expressed as mean ± SD. $^{\#}P < 0.05$, $^{\#\#}P < 0.01$ *vs.* normal group; $^{*}P < 0.05$, $^{**}P < 0.01$ *vs.* CIA group.

Information Fig. S5E), suggesting that endogenous PGE2-mediated signaling pathway involves in the regulation of FLS function in chronic arthritis, and CP-25 may improve FLS dysfunction by down-regulating PGE2 signaling pathway.

PGE2 levels were increased in synovial tissues of RA patients and AA rats[7,8,45,46]. Our study found that increased PGE2 levels in FLS of CIA rats may be mediate the up-regulation of GRK2 membrane expression, increase of GRK2 and EP4 co-localization, the down-regulation of EP4 membrane expression and decrease of EP4 receptor sensitivity for PGE2, thereby inducing synovial hyperplasia. CP-25 down-regulates GRK2 translocation, restores EP4 receptor sensitivity for PGE2, inhibiting synovial hyperplasia. Here, we hypothesized that the effect of CP-25 on FLS dysfunction is due to down-regulation of interaction between GRK2 and EP4. Firstly, we found that the abnormal proliferation of FLS in CIA group obviously strengthened compared with the control group, CP-25 and paroxetine significantly inhibit FLS abnormal proliferation (Fig. 3A). *In vitro*, Western blot (Fig. 3B) and flow cytometry (Fig. 3D and E) have been developed for detecting GRK2 and EP4 membrane and cytoplasm expression, found that GRK2 membrane expression and EP4 cytoplasm expression increased, GRK2 cytoplasm expression and EP4 membrane expression decreased in CIA group. CP-25 and paroxetine significantly down-regulated GRK2 translocation and restored EP4 membrane expression. Co-immunoprecipitate (Co-IP) combined with laser confocal microscopy was detected the

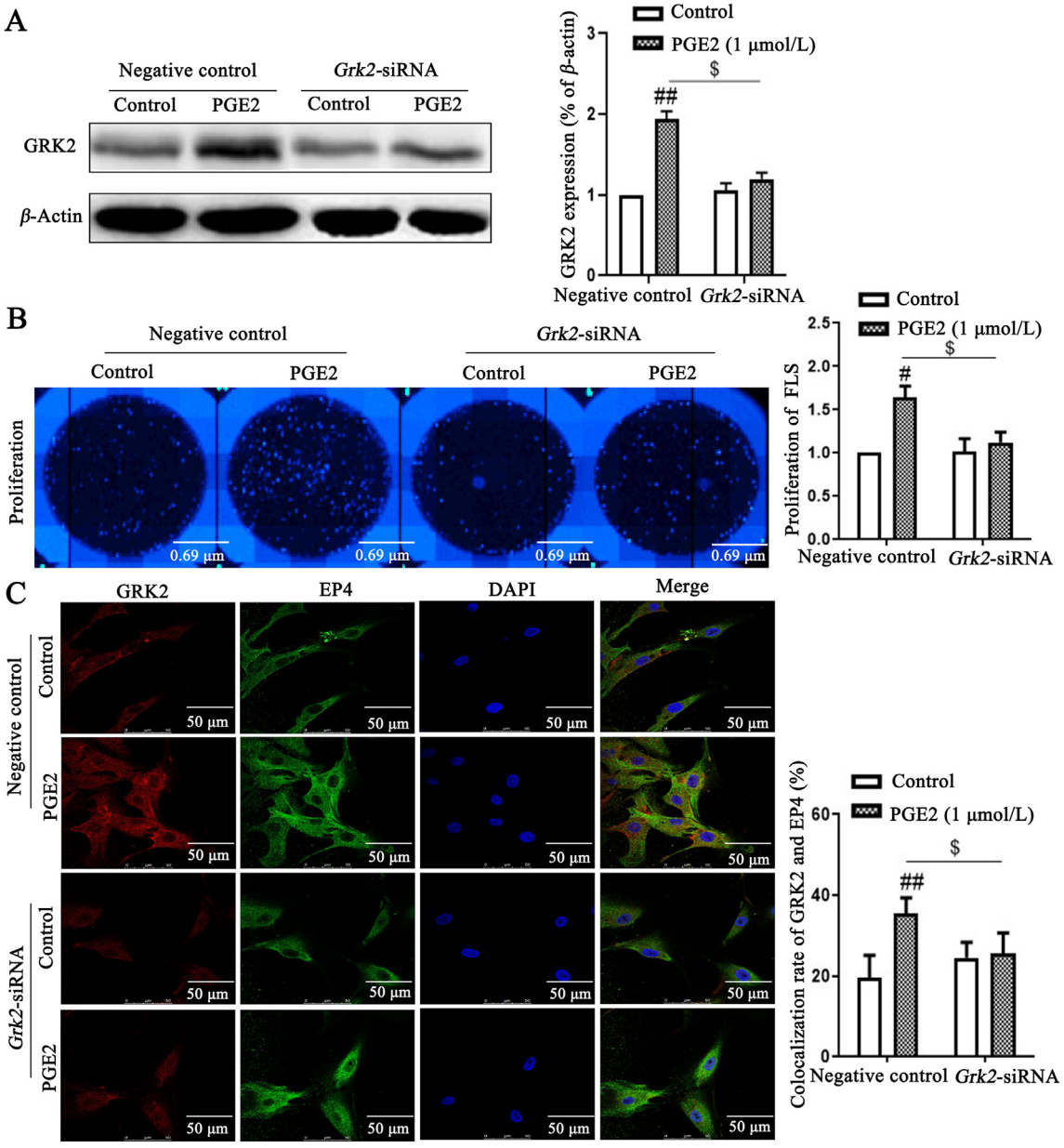

Figure 4 GRK2 knockdown strongly inhibits the proliferation of FLS, possibly *via* PGE2−EP4 signaling pathway. (A) *Grk2* siRNA was transfected into FLS, the inhibition rate of GRK2 was detected by Western blot ($n = 4$). (B) FLS proliferation was detected by high content cell imaging system images ($n = 6$). (C) The co-expression of GRK2 and EP4 was detected by laser confocal microscopy ($n = 6$). Scale bars = 50 μm. Data are expressed as mean ± SD. $^{\#}P < 0.05$, $^{\#\#}P < 0.01$ *vs.* control group; $^{\$}P < 0.05$ *vs.* negative control group with PGE2.

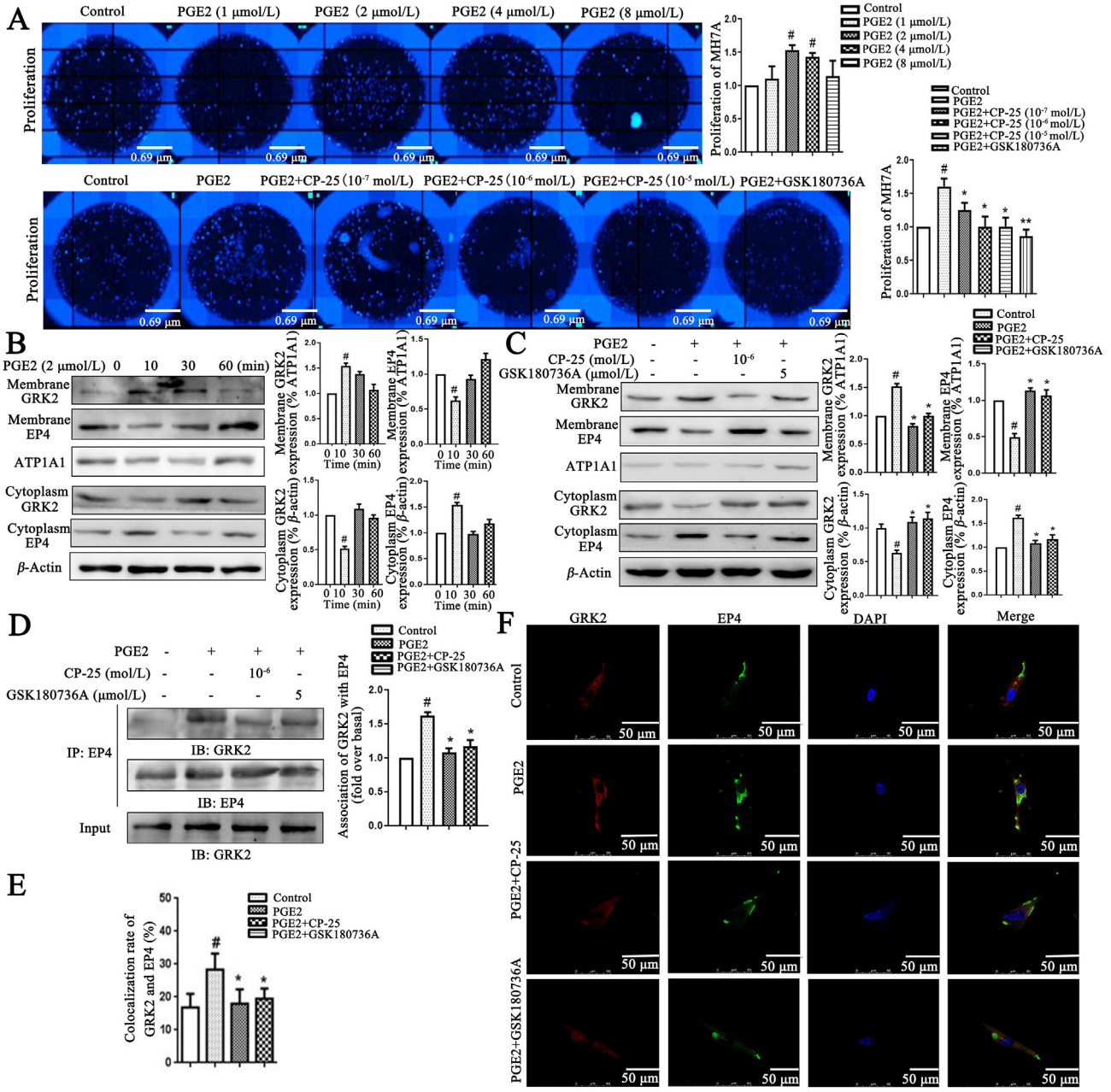

Figure 5 CP-25 inhibits PGE2-induced MH7A proliferation by down-regulating GRK2 translocation. (A) CP-25 inhibited PGE2-induced MH7A proliferation ($n = 3$). (B) PGE2 induced EP4 receptor short-term desensitization and GRK2 membrane translocation. The membrane expression of EP4 and GRK2 in MH7A treated by PGE2 were detected by Western blot ($n = 3$). (C) The effect of CP-25 on the expression of GRK2 and EP4 on membrane of MH7A stimulated by PGE2 ($n = 3$). (D) PGE2 stimulated MH7A lysates were used anti-EP4 antibody by co-immunoprecipitate and subjected to Western blot to visualize GRK2 to evaluate the association with EP4 ($n = 3$). (E) and (F) The co-expression of GRK2 and EP4 was detected by laser confocal microscopy ($n = 6$). Scale bars = 50 μm. Data are expressed as mean ± SD. $^{\#}P < 0.05$ *vs.* control group; $^{*}P < 0.05$, $^{**}P < 0.01$ *vs.* PGE2.

interaction and co-localization of GRK2 and EP4 (Fig. 3C and F), discovered that GRK2 and EP4 co-expression increased in CIA group, CP-25 and paroxetine down-regulated the co-expression. Above results suggested that CP-25 down-regulates GRK2 translocation to decrease the co-expression of GRK2 and EP4, and restore EP4 membrane expression, thereby improving FLS abnormal proliferation of CIA rats.

To further elucidate the functions of GRK2 in FLS, *Grk2* siRNA was transfected to knock down endogenous *Grk2* in FLS of CIA rats. *Grk2* siRNA, with high inhibition rate, were selected for further experiments (Fig. 4A). Exogenous PGE2 promoted FLS abnormal proliferation by up-regulating GRK2 translocation to EP4. Knockdown of *Grk2* significantly decreased PGE2-induced FLS proliferation (Fig. 4B), and down-regulated PGE2-induced

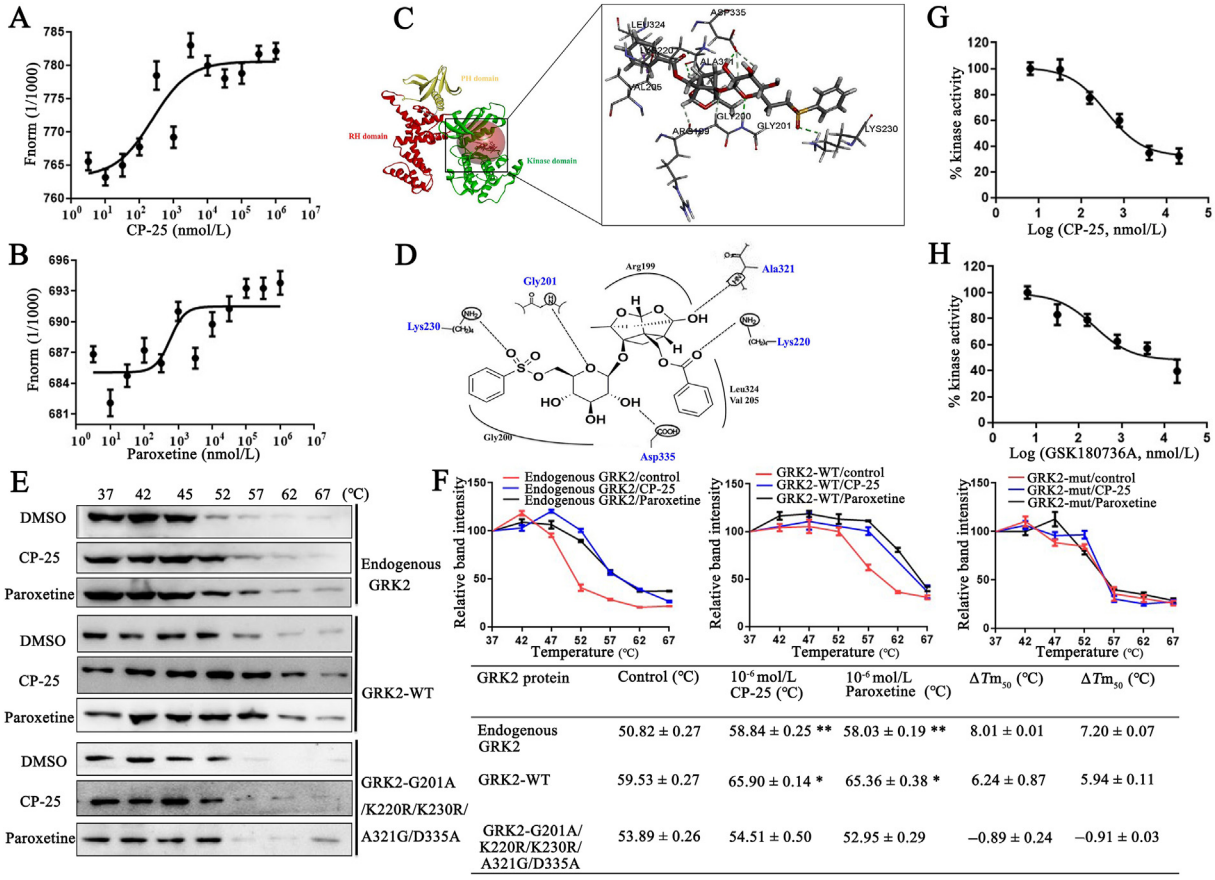

GRK2 protein	Control (℃)	10^{-6} mol/L CP-25 (℃)	10^{-6} mol/L Paroxetine (℃)	ΔTm_{50} (℃)	ΔTm_{50} (℃)
Endogenous GRK2	50.82 ± 0.27	58.84 ± 0.25 **	58.03 ± 0.19 **	8.01 ± 0.01	7.20 ± 0.07
GRK2-WT	59.53 ± 0.27	65.90 ± 0.14 *	65.36 ± 0.38 *	6.24 ± 0.87	5.94 ± 0.11
GRK2-G201A/ K220R/K230R/ A321G/D335A	53.89 ± 0.26	54.51 ± 0.50	52.95 ± 0.29	−0.89 ± 0.24	−0.91 ± 0.03

Figure 6 CP-25 directly binds to the kinase domain of GRK2 and inhibits GRK2 activity. (A) and (B) Microscale thermophoresis (MST) of CP-25 and paroxetine. GRK2 (0.49 mg/mL) were incubated with increasing concentrations of CP-25 (A) and paroxetine (B). The interactions of CP-25 or paroxetine and GRK2 were quantified by MST and binding data were plotted applying the K_d equation. (C) Molecular docking modeling of compound CP-25 and GRK2, the small molecule and the critical interaction of 3KRW are represented by sticks. Panel is a view into the active site cavity. (D) Schematic representation of the binding mode of CP-25 in the GRK2 binding site of 3KRW. (E) Cellular thermal shift assay (CETSA) presented the thermal stability of endogenous GRK2, wild-type GRK2 (GRK2-WT), and GRK2 G201A/A321G/D335A/K220R/K230R mutant proteins under treatment with CP-25 (10^{-6} mol/L) and paroxetine (10^{-6} mol/L). (F) CETSA curve and the thermal stability to reach 50% of temperature (Tm_{50}) value was performed using GraphPad Prism software. Data are expressed as mean ± SD. $^*P < 0.05$, $^{**}P < 0.01$ *vs.* control group. (G) and (H) Determining IC_{50} for CP-25 and GRK2 inhibitor. IC_{50} were determined using the ADP-Glo™ Kinase Assay. Curve fitting was performed using GraphPad Prism software. All data are expressed as mean ± SD.

the co-expression of GRK2 and EP4 (Fig. 4C). Taken together, GRK2 might be involved in PGE2-indued FLS abnormal proliferation.

To test the role of exogenous PGE2 induced MH7A (FLS line of patients with RA) abnormal proliferation and the effects of CP-25, we found that under the stimulation of PGE2, MH7A proliferation was increased, and PGE2-induced MH7A proliferation was reduced by CP-25 (Fig. 5A). To establish PGE2-induced EP4 short-term desensitization model, we first analyzed that Western blot has been developed for detecting GRK2 and EP4 membrane expression *in vitro*. When the GRK2 membrane expression was analyzed, it was increased continuously at 10 min but then gradually dropped, and decreased to the basal level at 1 h. However, EP4 membrane expression was decreased at 10 min, and was up to the basal level at 1 h (Fig. 5B), suggesting that GRK2 may be involved in EP4 desensitization. We further analyzed whether CP-25 was responsible for the regulation of GRK2 to affect EP4 desensitization. CP-25 significantly down-regulated GRK2 membrane expression and up-regulated EP4 membrane expression (Fig. 5C). Co-IP assay combined with laser confocal detecting GRK2 and EP4 co-expression showed that GRK2 and EP4 co-expression increased at 10 min by PGE2 stimulation, and CP-25 significantly down-regulates GRK2 and EP4 co-expression (Fig. 5D−F). Above results suggested that CP-25 inhibits FLS abnormal proliferation by down-regulating GRK2 transmembrane activity and promoting EP4 resensitization.

3.3. CP-25 directly binds to the kinase domain of GRK2 and inhibits GRK2 activity

To further study whether CP-25 directly affect GRK2 translocation, we determined K_d between CP-25 or paroxetine and GRK2 by MST. This method allows the determination of K_d values in solution and requires GRK2 to be fluorescently labeled. MST experiments were performed with increasing concentrations of each of CP-25 or paroxetine (dilutions from 5 nmol/L to 1 mmol/L) with a constant amount of GRK2 protein. The results indicated that increasing amounts of CP-25 and paroxetine clearly affect the thermophoretic motion of GRK2, CP-25 and paroxetine binding to GRK2 protein yielded K_d values of 1.75±0.38 and

4.95±1.26 μmol/L, respectively (Fig. 6A and B). The results showed that the combining capacity in the order of CP-25>paroxetine.

Next, we investigated the binding site of CP-25 acting on GRK2. Since CP-25 showing to target the GRK2 protein and no references could be used to speculate the binding mode, molecular docking of CP-25 into binding site of GRK2 was performed to simulate a binding model derived from GRK2 (3KRW.pdb). The docking simulation showed the binding model and sites of compound CP-25 with GRK2 complex (Fig. 6C). CP-25 bind to the kinase domain of GRK2 with R199, G200, G201, V205, K220, K230, A321, L324, and D335. Benzoyl side chain of CP-25 mainly combine with V205, K220, and L324 in the small lobe, cyclohexane and two oxygen heterocyclic rings mainly combine with R199 and A321 in P-loop, benzene sulfonyl side chain mainly combines with G200, G201, K230, and D335 in the large lobe, especially K230 in αB−αC-loop of GRK2. Visual inspection of the pose of CP-25 into the GRK2-site revealed that optimal hydrogen bond is observed. In the flexible binding simulation, five residues of GRK2, G201, K220, K230, A321, and D335 could form hydrogen bonds with the small-molecule ligand CP-25 to stabilize the binding conformation, which is important for the potent inhibitory activity of CP-25 (Fig. 6D).

Using site-directed mutagenesis, we constructed G201A/K220R/K230R/A321G/D335A mutant of GRK2. Moreover, CETSA with HepG2 cells demonstrated that CP-25 largely improved the thermal stability of GRK2, indicating the binding of CP-25 with GRK2. Exogenous wild-type GRK2 (GRK2-WT) showed a similar thermal stability shift under treatment of CP-25, while CP-25 did not change the thermal stability of exogenous GRK2-G201A/K220R/K230R/A321G/D335A, indicating G201, K220, K230, A321, and D335 might be responsible for the interaction between GRK2 and CP-25 (Fig. 6E and F), as predicted by molecular docking.

To determine whether CP-25 can regulate GRK2 activity, GRKtide (CRRREEEEESAAA) fragment was used as substrates in *in vitro* kinase reactions. Luminescence based GRK2 kinase activity measurement was done by ADP-Glo™ kinase assay kit. The maximum GRK2 activity was assessed without any inhibitor was kept as negative control. CP-25 and GSK180736A, an inhibitor of GRK2, at various concentrations ranging from 0.032 to 100 μmol/L, 50% GRK2 inhibition was observed. According to the experiment, half maximal inhibitory concentration (IC_{50}) of CP-25 and GSK180736A were observed to be 236.4 and 390.0 nmol/L, respectively. The results of kinase assay are represented graphically as percentage inhibition of kinase activity in comparison with the maximum kinase activity (Fig. 6G and H).

3.4. CP-25 may regulate GRK2 transmembrane by controlling Ala321 of GRK2

Using site-directed mutagenesis, we constructed some different GRK2 mutants including G201A, K220R, K230R, A321G, D335A, and G201A/K220R/K230R/A321G/D335A. In order to tell whether the CP-25 binding to GRK2 modulated the action of GRK2 in cells, we determined the interaction of GRK2 and EP4 under CP-25 and GSK180736A treatment. Using WT and mutants of GRK2 transiently transfected to HEK 293T cells for 48 h, the association of GRK2 and EP4 was detected by conventional methods such as co-IP assays. In HEK 293T cells, approx. 50% of the association of GRK2-WT and EP4 was contributed by PGE2 and CAY10598 (EP4 agonists). In the present study, we observed that the presence of the CP-25 (10^{-6} mol/L) and GRK2 inhibitor GSK180736A (5 μmol/L) inhibited agonists induced the association of GRK2-WT and EP4 (Fig. 7A).

Molecular docking assay showed that G201, K220, K230, A321, and D335 in kinase domain of GRK2 formed hydrogen bonds with CP-25. To confirm and extend these observations, we generated a wide range of single mutations within GRK2 kinase domain (Fig. 7H). G201A, K220R, K230R, A321G, and D335A caused significant decreasing of GRK2 translocation to EP4, approx. 30% of the association of GRK2 and EP4 was contributed by EP4 agonists. Notably, CP-25 and GSK180736A without significantly effect on GRK2-A321G translocation to EP4, but they decrease GRK2 mutants (G201A, K220R, K230R, and D335A) transmembrane (Fig. 7B−F). Thereby, A321 of GRK2 may be a key amino acid for CP-25 to regulate GRK2 translocation to EP4 receptor.

To further confirm the results, we did multiple mutations within GRK2 kinase domain (G201A/A321G/D335A/K220R/K230R). The results showed that GRK2 mutants combined with EP4 under the treatment of EP4 agonists, and CP-25 and GSK180736A did not affect GRK2 mutants translocation to EP4 receptor (Fig. 7G), which further suggesting that Ala321 of GRK2 play an important role in mediating GRK2 binding to EP4 receptor.

4. Discussion

Joint destruction is one of the most typical pathological hallmarks of RA. FLS contribute to joint destruction through increasing cell density of FLS and releasing inflammatory factors. Established CIA model of rats and collected synovial tissue of RA patients, GRK2 expression increased, the co-localization of GRK2 and EP4 increased, and EP4 expression decreased in synovial tissue of CIA rats and RA patients, suggesting that GRK2 translocation is related to synovial hyperplasia. Then, differential proteins from FLS of CIA rats were detected by label analysis, discovered that 33 differential proteins of FLS participate in regulating joint inflammation, synoviocytes dysfunction and the release of PGE2, TNF-α, IL-1β, IL-6, etc.[39−44], and we also found that FLS of CIA rats have an increased ability to secrete inflammatory factors including PGE2, TNF-α, IL-1β, IL-6, IFN-γ, etc. PGE2, as a vital inflammatory factor, highly expresses in the serum and synovial fluid of RA patients and AA rats, and involves in FLS abnormal proliferation[7,8,45,46], which is consistent with our current findings. Under normal physiological conditions, PGE2 also binding to EP4, activates cAMP−PKA signaling pathway, and regulates EP4 phosphorylation to keep the balance of cells and exert the regulatory of cell functions. However, sustained PGE2 stimulation is harmful effects over time, causing EP4 over-desensitization and decrease of EP4 sensitivity for PGE2, and further synovial cells dysfunction[7,47−50]. Here, we show that GRK2 translocation to EP4 is increased in FLS during arthritis, promoting the association of GRK2 and EP4, leading to EP4 desensitization, thereby inducing FLS abnormal proliferation. To further identify the role of GRK2 in FLS abnormal proliferation, the silencing of GRK2 blocks PGE2-induced FLS abnormal proliferation. These findings suggested that GRK2 might be a novel potential therapeutic target for regulating FLS abnormal proliferation of RA.

GRK2, as a vital Ser/Thr kinase, is widely distributed in different tissues, its activity and expression might be modulated by interactions with protein and lipid in specific cell types, which

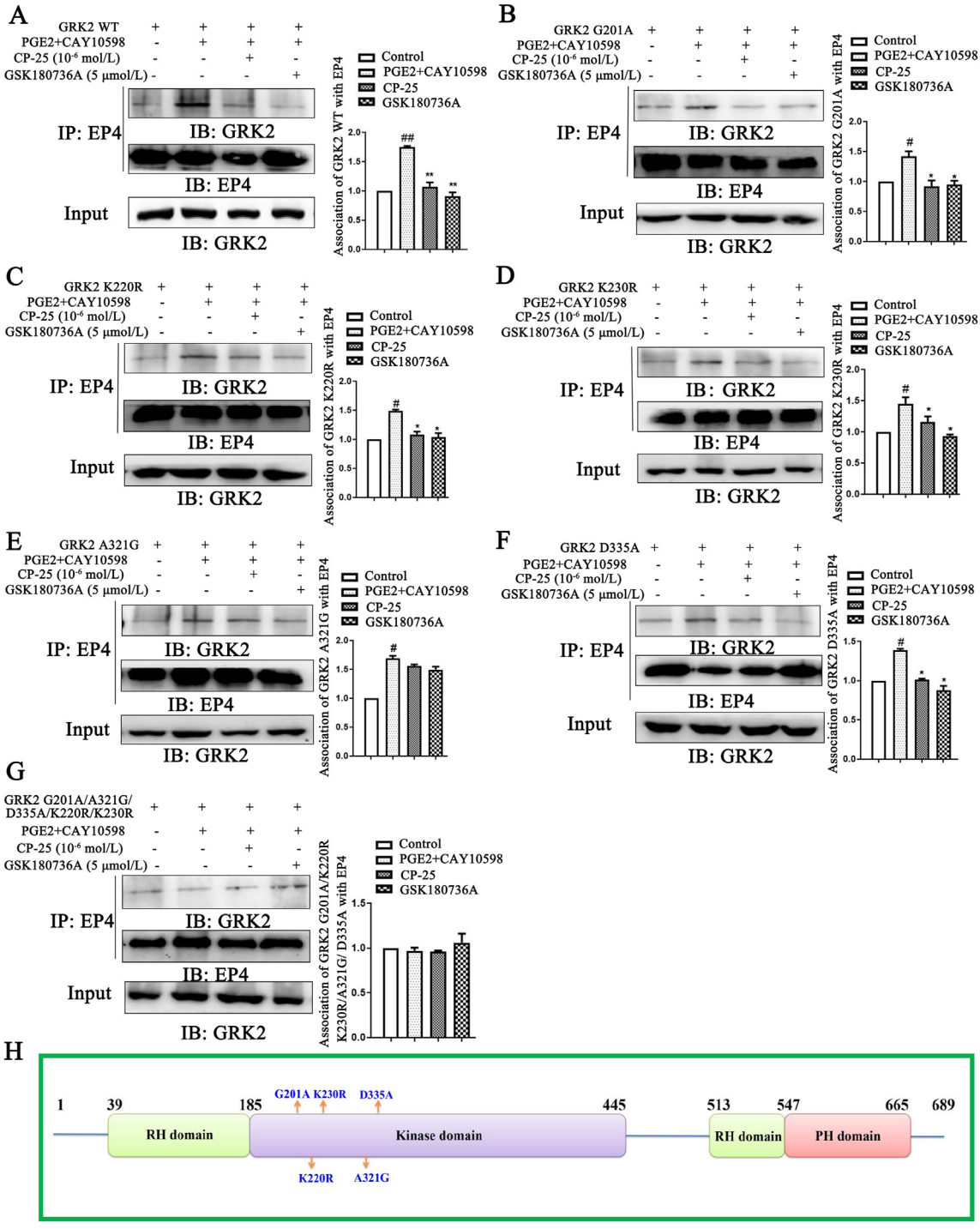

Figure 7 Study on the binding sites of CP-25 and GRK2. HEK 293T cells transfection with pIRES-EGFP-GRK2 WT (A), pIRES-EGFP-GRK2 G201A (B), pIRES-EGFP-GRK2 K220R (C), pIRES-EGFP-GRK2 K230R (D), pIRES-EGFP-GRK2 A321G (E), pIRES-EGFP-GRK2 D335A (F), and pIRES-EGFP-GRK2 G201A/K220R/K230R/A321G/D335A (G) plasmids were challenged with CAY10598 (1 μmol/L) following a 1 h pre-treatment with PGE2 (10 μmol/L) for 30 min in the presence and absence of CP-25 (10^{-6} mol/L) or GSK180736A (5 μmol/L). The association of GRK2 mutants and EP4 was determined by co-IP using the EP4-specific antibody and subsequent blotting with GRK2-specific ($n = 3$). Data are expressed as mean ± SD. $^{\#}P < 0.05$, $^{\#\#}P < 0.01$ *vs.* control group; $^{*}P < 0.05$, $^{**}P < 0.01$ *vs.* PGE2+CAY10598 group. (H) Location of mutations made in the GRK2 domain. Light green bars represent the regulator of G-protein signaling (RGS) homology (RH) domain, light purple bars represent kinase domain and pink bars represent Pleckstrin homology (PH) domain. G201, K220, K230, A321, and D335 residues are those that were mutated in this study.

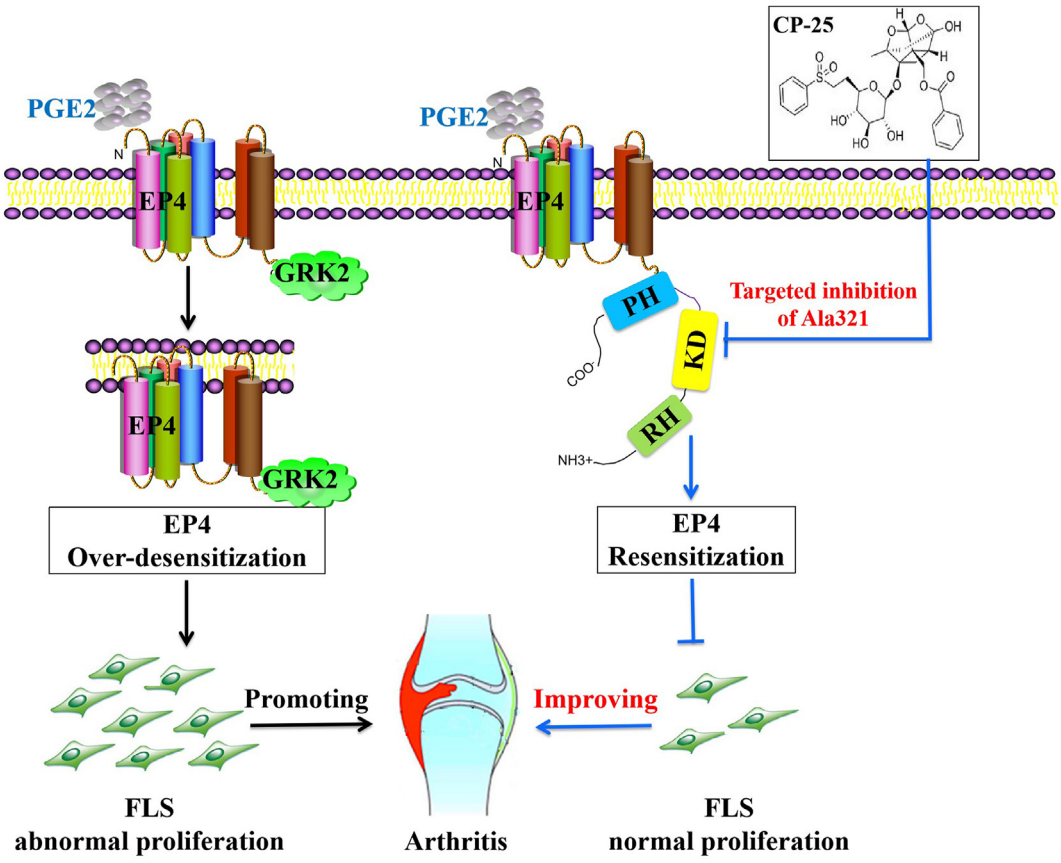

Figure 8 Schematic illustration of CP-25 improves EP4 desensitization mediated FLS dysfunction *via* stabilizing KD and controlling Ala321 of GRK2. PGE2 level in FLS of CIA rats was up-regulated, promoting PGE2 binding to the EP4 receptor, inducing the increasing of GRK2 translocation, leading to EP4 over-desensitization, thereby promoting FLS dysfunction. CP-25 can stabilize the kinase domain of GRK2 to directly inhibit GRK2 kinase, leading to decreasing of GRK2 translocation to EP4 by controlling Ala321 of GRK2, thereby promoting EP4 resensitization, which was an important mechanism of CP-25 in improving FLS dysfunction.

would be also critical to unveil key cellular and physiological processes controlled by this protein. It has been reported that increased GRK2 levels and/or activity may play an important role in the development of diseases, such as relevant cardiovascular, hypertension, inflammatory, cancer pathologies, and so on[51]. Structural analysis of GRK2 indicated that it includes N-terminal domain (1−184 aa), kinase domain (185−513 aa), and C-terminal domain (514−689 aa). KD of GRK2 included the small lobe (186−272 aa, 496−513 aa), hinge region (273−275 aa), the large lobe (276−495 aa), P-loop (191−201 aa), the activation loop (contains Ser334), and αB−αC-helix (224−248 aa), which was the binding regions of ATP and GRK2 inhibitors[52,53]. The structural features of GRK2 play a vital role in the development of GRK2 inhibitors.

GRK2 inhibitors have been classified several types according to the different inhibition mechanisms. Such as, ATP mimetic and competitive inhibitor of ATP (Balanol) combined specifically with the P-loop and the αB−αC loop of the small lobe in GRK2, leading to kinase domain of GRK2 adopted a slightly more closed conformation[54]. Heterocyclic compounds Takeda inhibitors (CMPD101 and CMPD103A) specifically bind to the active site of GRK2 including the large lobe, the P-loop, and the αB−αC-loop to stabilize non-active conformation with higher selectivity than Balanol[55]. Paroxetine and derivatives (GSK180736A) specifically integrated with the kinase domain of GRK2 by forming hydrogen bonds at D272 and M274 to inhibit kinase activity[38]. Notably, there have been a number of recent advances in GRK2 inhibitors for treating cardiovascular, hypertension of animals. Especially, paroxetine is a well-known antidepressant in clinic, and inhibits GRK2 and increase β-adrenergic receptor (β-AR) mediated cardiomyocyte contractility in normal mice and cells[56−60]. However, the role of GRK2 inhibitors in treating RA remains unidentified.

CP-25, as a novel ester derivative of paeoniflorin, has anti-inflammation and immunoregulation effects on CIA rats. CP-25 and GRK2 inhibitors improve the FLS abnormal proliferation by down-regulating GRK2 translocation. *In vitro*, MST combined with molecular docking found that CP-25 directly binds to GRK2 protein, kinase domain of GRK2 is the binding region of CP-25, especially, the small lobe, P-loop, the large lobe, and αB−αC-loop of kinase domain in GRK2 are the important binding domains of CP-25, and CP-25 makes hydrogen bonds to G201, K220, K230, A321, and D335 of kinase domain to stabilize CP-25/GRK2 complex. Cellular thermal shift assay found that CP-25 can bind and stabilize GRK2 protein in cells. To further explore the effects of CP-25 on GRK2 functions, we detected the GRK2 activity and the ability of GRK2 to interact with EP4

receptor in the presence of CP-25 by transfecting with GRK2-WT, G201A, K220R, K230R, A321G, D335A, and G201A/A321G/D335A/K220R/K230R. Therefore, CP-25, as activity regulator of GRK2, targets to GRK2 thereby down-regulating the association of GRK2 and EP4 and mediating EP4 resensitization by controlling the key amino acid Ala321 of GRK2.

Currently, selective inhibitors targeting key molecules for treating RA in clinic include celecoxib (cyclooxygenase-2 inhibitors), etanercept (TNF-α inhibitors), rituximab (CD20 monoclonal antibody), tocilizumab (IL-6R monoclonal antibody), and so on. However, ADR would occur under the conditions of inhibiting excessively molecules in FLS and immune cells, which may induce malignant tumors, infections, myelosuppression, and so on. In this study, CP-25 relieves the FLS abnormal proliferation, involving in the down-regulation of GRK2 membrane expression, decrease of GRK2 and EP4 co-localization, thereby restoring EP4 membrane expression in FLS to normal level, which achieve the soft regulation of inflammatory immune responses (SRIIR) of drug and represent an innovate avenue for the development of new therapeutic strategy against RA[61].

5. Conclusions

This study provides strong evidence that GRK2 translocation to EP4 contributes to the regulation of EP4 over-desensitization in synovial tissues and FLS of RA patients and CIA rats by PGE2−EP4 signaling pathway, mediating FLS abnormal proliferation, which suggest that GRK2 might be a potential biomarker and attractive therapeutic target for RA. CP-25 directly targets GRK2, regulates EP4 receptor over-desensitization to normal physiological level, re-establishes EP4 signaling pathway functions and thereby inhibiting FLS abnormal proliferation (Fig. 8). Therefore, CP-25 is worthy to be applied in the treatment of RA in clinic in the future.

Acknowledgments

We thank Drs. Qingsong Liu and Ao'li Wang from Chinese Academy of Sciences for materials and MST technical assistance, Drs. Xinhua Liu from Anhui Medical University for molecular docking technical assistance. This research was supported by the Key Project of National Natural Science Foundation of China (No. 81330081), Surface Project of National Natural Science Foundation of China (No. 81673444), and Youth Science Fund Project of National Natural Science Foundation of China (No. 81502123).

Author contributions

Chenchen Han participated in the design of the study and performed most of the experiments, statistical analysis, and wrote the manuscript. Yifan Li, Yuwen Zhang, Yang Wang, Dongqian Cui, Tingting Luo, Yu Zhang, Qian Liu, Hao Li, and Chun Wang performed the experiments. Yang Ma, Dexiang Xu, and Wei Wei conceived the study and revised the manuscript. All authors approved the final version of the manuscript to be published.

Conflicts of interest

The authors have no financial conflicts of interest.

Appendix A. Supporting information

Supporting data to this article can be found online at https://doi.org/10.1016/j.apsb.2021.01.015.

References

1. Cross M, Smith E, Hoy D, Carmona L, Wolfe F, Vos T, et al. The global burden of rheumatoid arthritis: Estimates from the Global Burden of Disease 2010 study. *Ann Rheum Dis* 2014;**73**:1316−22.
2. Benson RA, McInnes IB, Brewer JM, Garside P. Cellular imaging in rheumatic diseases. *Nat Rev Rheumatol* 2015;**11**:357−67.
3. Schumacher HR. Are we being open enough to all approaches to therapy of rheumatoid arthritis?. *J Clin Rheumatol* 2013;**19**:167−71.
4. Lee DM, Kiener HP, Agarwal SK, Noss EH, Watts GFM, Chisaka O, et al. Cadherin-11 in synovial lining formation and pathology in arthritis. *Science* 2007;**315**:1006−10.
5. Chen Q, Wei W. Effects and mechanisms of glucosides of chaenomeles speciosa on collagen-induced arthritis in rats. *Int Immunopharm* 2003;**3**:593−608.
6. Zhang LL, Wei W, Wang NP, Wang QT, Chen JY, Chen Y, et al. Paeoniflorin suppresses inflammatory mediator production and regulates G protein-coupled signaling in fibroblast-like synoviocytes of collagen induced arthritic rats. *Inflamm Res* 2008;**57**:388−95.
7. Jia X, Chang Y, Wei F, Dai X, Wu Y, Sun X, et al. CP-25 reverses prostaglandin E4 receptor desensitization-induced fibroblast-like synoviocyte dysfunction *via* the G protein-coupled receptor kinase 2 in autoimmune arthritis. *Acta Pharmacol Sin* 2019;**40**:1029−39.
8. Yang X, Zhao Y, Jia X, Wang C, Wu Y, Zhang L, et al. CP-25 combined with MTX/LEF ameliorates the progression of adjuvant-induced arthritis by the inhibition on GRK2 translocation. *Biomed Pharmacother* 2019;**110**:834−43.
9. Wang Y, Han C, Cui D, Luo T, Li Y, Zhang Y, et al. Immunomodulatory effects of CP-25 on splenic T cells of rats with adjuvant arthritis. *Inflammation* 2018;**41**:1049−63.
10. Aragay AM, Mellado M, Frade JM, Martin AM, Jimenez-Sainz MC, Martinez -AC, et al. Monocyte chemoattractant protein-1-induced CCR2B receptor desensitization mediated by the G protein-coupled receptor kinase 2. *Proc Natl Acad Sci U S A* 1998;**95**:2985−90.
11. Murga C, Ruiz-Gómez A, García-Higuera I, Kim CM, Benovic JL, Mayor Jr F. High affinity binding of beta-adrenergic receptor kinase to microsomal membranes. *J Biol Chem* 1996;**2**:985−94.
12. Carman CV, Parent JL, Day PW, Pronin AN, Sternweis PM, Wedegaertner PB, et al. Selective regulation of Galpha(q/11) by an RGS domain in the G protein-coupled receptor kinase. *GRK2. J Biol Chem* 1999;**274**:34483−92.
13. Penela P, Murga C, Ribas C, Lafarga V, Mayor Jr F. The complex G protein-coupled receptor kinase 2 (GRK2) interactome unveils new physiopathological targets. *Br J Pharmacol* 2010;**160**:821−32.
14. Wang Q, Wang L, Wu L, Zhang M, Hu S, Wang R, et al. Paroxetine alleviates T lymphocyte activation and infiltration to joints of collagen-induced arthritis. *Sci Rep* 2017;**77**:45364.
15. Visser K, van der Heijde D. Optimal dosage and route of administration of methotrexate in rheumatoid arthritis: A systematic review of the literature. *Ann Rheum Dis* 2009;**68**:1094−9.
16. Hoekstra M, van Ede AE, Haagsma CJ, van de Laar MA, Huizinga TW, Kruijsen MW, et al. Factors associated with toxicity, final dose, and efficacy of methotrexate in patients with rheumatoid arthritis. *Ann Rheum Dis* 2003;**62**:423−6.
17. Morgan SL, Baggott JE, Bernreuter WK, Gay RE, Arani R, Alarcón GS. MTX affects inflammation and tissue destruction differently in the rat AA model. *J Rheumatol* 2001;**28**:1476−81.
18. Liu DY, Lon HK, Wang YL, DuBois DC, Almon RR, Jusko WJ. Pharmacokinetics, pharmacodynamics and toxicities of methotrexate in healthy and collagen-induced arthritic rats. *Biopharm Drug Dispos* 2013;**34**:203−14.

19. Burmester GR, Feist E, Dörner T. Emerging cell and cytokine targets in rheumatoid arthritis. *Nat Rev Rheumatol* 2014;**10**:77−88.
20. Sfikakis PP, Tsokos GC. Towards the next generation of anti-TNF drugs. *Clin Immunol* 2011;**141**:231−5.
21. Fleischmann R, Kremer J, Cush J, Schulze-Koops H, Connell CA, Bradley JD, et al. Placebo-controlled trial of tofacitinib monotherapy in rheumatoid arthritis. *N Engl J Med* 2012;**6**:495−507.
22. Atzeni F, Batticciotto A, Masala IF, Talotta R, Benucci M, Sarzi-Puttini P. Infections and biological therapy in patients with rheumatic diseases. *Isr Med Assoc J* 2016;**18**:164−7.
23. Davies R, Southwood TR, Kearsley-Fleet L, Lunt M, Hyrich KL. Medically significant infections are increased in patients with juvenile idiopathic arthritis treated with etanercept: Results from the British Society for Paediatric and Adolescent Rheumatology Etanercept Cohort Study. *Arthritis Rheumatol* 2015;**67**:2487−94.
24. Wang C, Yuan J, Zhang LL, Wei W. Pharmacokinetic comparisons of Paeoniflorin and paeoniflorin-6′*O*-benzene sulfonate in rats *via* different routes of administration. *Xenobiotica* 2016;**46**:1142−50.
25. Yang XD, Wang C, Zhou P, Yu J, Asenso J, Ma Y, et al. Absorption characteristic of paeoniflorin-6′-*O*-benzene sulfonate (CP-25) in *in situ* single-pass intestinal perfusion in rats. *Xenobiotica* 2016;**46**:775−83.
26. Chang Y, Jia X, Wei F, Wang C, Sun X, Xu S, et al. CP-25, a novel compound, protects against autoimmune arthritis by modulating immune mediators of inflammation and bone damage. *Sci Rep* 2016;**6**:26239.
27. Zhang F, Shu J, Li Y, Wu Y, Zhang X, Han L, et al. CP-25, a novel anti-inflammatory and immunomodulatory drug, inhibits the functions of Activated human B cells through regulating BAFF and TNF-alpha signaling and comparative efficacy with biological agents. *Front Pharmacol* 2017;**8**:933.
28. Shu JL, Zhang XZ, Han L, Zhang F, Wu YJ, Tang XY, et al. Paeoniflorin-6′-*O*-benzene sulfonate alleviates collagen-induced arthritis in mice by downregulating BAFF−TRAF2−NF-κB signaling: Comparison with biological agents. *Acta Pharmacol Sin* 2019;**40**:801−13.
29. Wang Q, Zhang L, Wu H, Wei W. The expression change of β-arrestins in fibroblast-like synoviocytes from rats with collagen-induced arthritis and the effect of total glucosides of paeony. *J Ethnopharmacol* 2011;**133**:511−6.
30. Huang B, Wang QT, Song SS, Wu YJ, Ma YK, Zhang LL, et al. Combined use of etanercept and MTX restores $CD4^+/CD8^+$ ratio and Tregs in spleen and thymus in collagen-induced arthritis. *Inflamm Res* 2012;**61**:1229−39.
31. Chang Y, Wu Y, Wang D, Wei W, Qin Q, Xie G, et al. Therapeutic effects of TACI-Ig on rats with adjuvant-induced arthritis *via* attenuating inflammatory responses. *Rheumatology* 2011;**50**:862−70.
32. Li P, Liu D, Liu Y, Song S, Wang Q, Chang Y, et al. BAFF/BAFF-R involved in antibodies production of rats with collagen-induced arthritis *via* PI3K−Akt−mTOR signaling and the regulation of paeoniflorin. *J Ethnopharmacol* 2012;**141**:290−300.
33. Han CC, Liu Q, Zhang Y, Li YF, Cui DQ, Luo TT, et al. CP-25 inhibits PGE2-induced angiogenesis by down-regulating EP4/AC/-cAMP/PKA-mediated GRK2 translocation. *Clin Sci (Lond)* 2020;**134**:331−47.
34. Guo X, Ji J, Feng Z, Hou X, Luo Y, Mei Z. A network pharmacology approach to explore the potential targets underlying the effect of sinomenine on rheumatoid arthritis. *Int Immunopharm* 2020;**80**:106201.
35. Liu F, Wang B, Wang Q, Qi Z, Chen C, Kong LL, et al. Discovery and characterization of a novel potent type II native and mutant BCR-ABL inhibitor (CHMFL-074) for Chronic Myeloid Leukemia (CML). *Oncotarget* 2016;**7**:45562−74.
36. Wu X, Huang C, Jia Y, Song B, Li J, Liu X. Novel coumarin-dihydropyrazole thio-ethanone derivatives: Design, synthesis and anticancer activity. *Eur J Med Chem* 2014;**74**:717−25.
37. Lin J, Yu Y, Wang X, Ke Y, Sun C, Yue L, et al. Iguratimod inhibits the aggressiveness of rheumatoid fibroblast-like synoviocytes. *J Immunol Res* 2019;**2019**:6929286.
38. Waldschmidt HV, Homan KT, Cruz-Rodríguez O, Cato MC, Waninger-Saroni J, Larimore KM, et al. Structure-based design, synthesis, and biological evaluation of highly selective and potent G protein-coupled receptor kinase 2 inhibitors. *J Med Chem* 2015;**59**:3793−807.
39. Biscetti F, Flex A, Alivernini S, Tolusso B, Gremese E, Ferraccioli G. The role of high-mobility group box-1 and its crosstalk with microbiome in rheumatoid arthritis. *Mediators Inflamm* 2017;**2017**:5230374.
40. Garcia-Arellano S, Hernandez-Palma LA, Bucala R, Hernandez-Bello J, De la Cruz-Mosso U, Garcia-Iglesias T, et al. Th1/Th17 cytokine profile is induced by macrophage migration inhibitory factor in peripheral blood mononuclear cells from rheumatoid arthritis patients. *Curr Mol Med* 2018;**18**:679−88.
41. Jenkins E, Brenner M, Laragione T, Gulko PS. Synovial expression of Th17-related and cancer-associated genes is regulated by the arthritis severity locus Cia10. *Gene Immun* 2012;**13**:221−31.
42. Katano M, Okamoto K, Arito M, Kawakami Y, Kurokawa MS, Suematsu N, et al. Implication of granulocyte-macrophage colony-stimulating factor induced neutrophil gelatinase-associated lipocalin in pathogenesis of rheumatoid arthritis revealed by proteome analysis. *Arthritis Res Ther* 2009;**11**:R3.
43. Lee JY, Kang MJ, Choi JY, Park JS, Park JK, Lee EY, et al. Apolipoprotein B binds to enolase-1 and aggravates inflammation in rheumatoid arthritis. *Ann Rheum Dis* 2018;**77**:1480−9.
44. Xu CP, Li X, Hu YJ, Cui Z, Wang L, Liang L, et al. Quantitative proteomics reveals ELP2 as a regulator to the inhibitory effect of TNF-α on osteoblast differentiation. *J Proteomics* 2015;**114**:234−46.
45. Kojima F, Naraba H, Sasaki Y, Beppu M, Aoki H, Kawai S. Prostaglandin E2 is an enhancer of interleukin-1β-induced expression of membrane-associated prostaglandin E synthase in rheumatoid synovial fibroblasts. *Arthritis Rheum* 2003;**48**:2819−28.
46. Largo R, Diez-Ortego I, Sanchez-Pernaute O, Lopez-Armada MJ, Alvarez-Soria MA, Egido J, et al. EP2/EP4 signalling inhibits monocyte chemoattractant protein-1 production induced by interleukin 1beta in synovial fibroblasts. *Ann Rheum Dis* 2004;**63**:1197−204.
47. Salazar NC, Chen J, Rockman HA. Cardiac GPCRs: GPCR signaling in healthy and failing hearts. *Biochim Biophys Acta* 2007;**1768**:1006−18.
48. Mann DL. Mechanisms and models in heart failure. *Circulation* 1999;**100**:999−1008.
49. Rockman HA, Koch WJ, Lefkowitz RJ. Seven-transmembrane-spanning receptors and heart function. *Nature* 2002;**415**:206−12.
50. Tilley DG, Rockman HA. Role of β-adrenergic receptor signaling and desensitization in heart failure: New concepts and prospects for treatment. *Expert Rev Cardiovasc Ther* 2014;**4**:417−32.
51. Han C, Li Y, Wang Y, Cui D, Luo T, Zhang Y, et al. Development of inflammatory immune response-related drugs based on G protein-coupled receptor kinase 2. *Cell Physiol Biochem* 2018;**51**:729−45.
52. Homan KT, Larimore KM, Elkins JM, Szklarz M, Knapp S, Tesmer JJG. Identification and structure−function analysis of subfamily selective G protein-coupled receptor kinase inhibitors. *ACS Chem Biol* 2014;**10**:310−9.
53. Thal DM, Yeow RY, Schoenau C, Huber J, Tesmer JJG. Molecular mechanism of selectivity among G protein-coupled receptor kinase 2 inhibitors. *Mol Pharmacol* 2011;**80**:294−303.
54. Tesmer JJG, Tesmer VM, Lodowski DT, Steinhagen H, Huber J. Structure of human G protein-coupled receptor kinase 2 in complex with the kinase inhibitor Balanol. *J Med Chem* 2010;**53**:1867−70.
55. Waldschmidt HV, Homan KT, Cato MC, Cruz-Rodríguez O, Cannavo A, Wilson MW, et al. Structure-based design of highly selective and potent G protein-coupled receptor kinase 2 inhibitors based on paroxetine. *J Med Chem* 2017;**60**:3052−69.
56. Abd Alla J, Graemer M, Fu X, Quitterer U. Inhibition of G-protein-coupled receptor kinase 2 prevents the dysfunctional cardiac substrate metabolism in fatty acid synthase transgenic mice. *J Biol Chem* 2016;**291**:2583−600.
57. Powell JM, Ebin E, Borzak S, Lymperopoulos A, Hennekens CH. Hypothesis: Paroxetine, a G protein-coupled receptor kinase 2 (GRK2)

inhibitor reduces morbidity and mortality in patients with heart failure. *J Cardiovasc Pharmacol Therapeut* 2016;**22**:51−3.
58. Schumacher SM, Gao E, Zhu W, Chen X, Chuprun JK, Feldman AM, et al. Paroxetine-mediated GRK2 inhibition reverses cardiac dysfunction and remodeling after myocardial infarction. *Sci Transl Med* 2015;**7**:231r−77r.
59. Thal DM, Homan KT, Chen J, Wu EK, Hinkle PM, Huang ZM, et al. Paroxetine is a direct inhibitor of G protein-coupled receptor kinase 2 and increases myocardial contractility. *ACS Chem Biol* 2012;**7**:1830−9.
60. Tian X, Wang Q, Guo R, Xu L, Chen Q, Hou Y. Effects of paroxetine-mediated inhibition of GRK2 expression on depression and cardiovascular function in patients with myocardial infarction. *Neuropsychiatric Dis Treat* 2016;**12**:2333−41.
61. Wei W. Soft regulation of inflammatory immune responses. *Chin Pharmacol Bull* 2016;**3**:297−303.